Armed Services Technical Information Agency

AD 208011

NOTICE: WHEN GOVERNMENT OR OTHER DRAWINGS, SPECIFICATIONS OR OTHER DATA ARE USED FOR ANY PURPOSE OTHER THAN IN CONNECTION WITH A DEFINITELY RELATED GOVERNMENT PROCUREMENT OPERATION, THE U. S. GOVERNMENT THEREBY INCURS NO RESPONSIBILITY, NOR ANY OBLIGATION WHATSOEVER; AND THE FACT THAT THE GOVERNMENT MAY HAVE FORMULATED, FURNISHED, OR IN ANY WAY SUPPLIED THE SAID DRAWINGS, SPECIFICATIONS, OR OTHER DATA IS NOT TO BE REGARDED BY IMPLICATION OR OTHERWISE AS IN ANY MANNER LICENSING THE HOLDER OR ANY OTHER PERSON OR CORPORATION, OR CONVEYING ANY RIGHTS OR PERMISSION TO MANUFACTURE, USE OR SELL ANY PATENTED INVENTION THAT MAY IN ANY WAY BE RELATED THERETO.

Reproduced by

DOCUMENT SERVICE CENTER

KNOTT BUILDING, DAYTON, 2, OHIO

UNCLASSIFIED

AD No. 20 801
ASTIA FILE COPY

THE SPLIT-FEEDBACK PUSH-PULL MAGNETIC AMPLIFIER

by

Isaac M. Horowitz

Research Report R-330-53, PIB-266
Office Of Naval Research
Contract NOnr-292(00), Proj. No.075-215

July 28, 1953

MRI

POLYTECHNIC INSTITUTE OF BROOKLYN
MICROWAVE RESEARCH INSTITUTE

Microwave Research Institute
Polytechnic Institute of Brooklyn
55 Johnson Street
Brooklyn 1, New York

Report R-330-53, PIB-266
Project Design NR-075-215

THE SPLIT-FEEDBACK PUSH-PULL MAGNETIC AMPLIFIER

by

Isaac M. Horowitz

Title Page
Acknowledgement
Abstract
Table of Contents
List of Symbols
35 Pages of Text
Appendix (3 Pages)
Bibliography
25 Pages of Figures

Contract NOnr-292(00)

Brooklyn 1, New York
July 28, 1953

ACKNOWLEDGEMENT

The study of Magnetic Amplifiers is being undertaken at the Microwave Research Institute of the Polytechnic Institute of Brooklyn under the sponsorship of the Office of Naval Research Contract NOnr-292(00).

The author gratefully acknowledges the generous advice, help and counsel of Doctor E.J. Smith and the encouragement and stimulation of Professor M.M. Liwschitz-Garik in his weekly conferences with the Magnetic Amplifier Group.

ABSTRACT

This report is devoted to the description and theoretical and experimental analysis of a new AC Phase-Sensitive (Push-Pull) Magnetic Amplifier, invented by the author, called the Split-Feedback Push-Pull Magnetic Amplifier.

In this new circuit, the feedback windings are split and arranged in such a manner that the amplification is high when load current flows and is very low when there is no load current (and circulating current flows).

This amplifier is compared in detail with the Voltage Doubler Push-Pull Magnetic Amplifier. Its principal advantage over the latter is its low circulating currents, which have a maximum rectified average value of one-half the maximum load current. The gain capabilities of the new amplifier are theoretically as great, and in practice, greater than those of the Doubler. In addition it has significant advantages over the Doubler with respect to sensitivity to variations in Bias or Line voltages, ease of Bias adjustment, and behavior in the saturated range. The price paid is a slight increase in complexity and the possibility that a larger number of rectifier discs may be needed.

It is suggested that the reader who is interested in conclusions, rather than details, read Sections I and VII and note Figures MRI-13397, MRI-13398, MRI-13400a thru 13400c, MRI-13412a, MRI-13412b, MRI-13413a, and MRI-13413b.

TABLE OF CONTENTS

TABLE OF CONTENTS (Continued)

SYMBOLS

As each symbol is introduced it is defined in the report or in the figures and thereafter used with no further comment. In addition, a key to the symbols is herewith presented.

i_1, I_1; i_2, I_2; - mesh currents

i, I; - load currents

I_1 I_2 I_m etc. - rectified average values of currents

$\bar{I}_c$ $\bar{I}_b$ etc. - true average values of currents

I_m - maximum rectified average load current = $(2/\pi)(V_m/R_t)$

I'_m - maximum rectified average circulating current = $\frac{2}{\pi} \frac{V_m}{r}$

i_b, I_b; i_c, I_c; - bias and control currents respectively

I_x - a circuit parameter = $2\ (N_b/N)\ I_b$

N_c, N_b, N; - control, bias and load core turns

R_t - total mesh resistance

R - that portion of the mesh resistance which is common to both meshes, i.e., the load resistance.

r - that portion of the mesh resistance which is not common to both meshes. $R_t = R + r$.

V_m - peak value of applied voltage per mesh

V_{sm} - peak value of minimum AC voltage which saturates a core of N turns

Φ_m - magnetic flux in webers = V_m/wN

Φ_s - magnetic flux in webers .....V_{sm}/wN

$d = b$ - a circuit parameter, whose value = $1 + R/R_t$

I. Push-Pull Magnetic Amplifier Types and the Problem of Excess Currents

This report is concerned with magnetic amplifiers whose output is an AC signal, (at excitation frequency), phase-sensitive to the polarity of the input DC (or low frequency) signal, usually referred to as the AC Push-Pull Magnetic Amplifier.

A. Classification on the Basis of Load

Such amplifiers may be divided into two classes based on whether the load is or is not split and electrically isolated into a pair of 2-terminal loads. When such a split load is available, the Push-Pull circuit consists of two meshes (with half the load in each mesh), which are electrically isolated from each other (Fig. MRI-13389a); and so there are two simple circuits unaffected by the manner in which they are being used. No further comment need be made on this class.

The second class of Push-Pull Amplifiers consists of those where there is some coupling between the two meshes. This class includes two-terminal loads as such, (Fig. MRI-13389b), split loads with coupling between the two parts, as well as 2-terminal loads with mixing resistors (Fig. MRI-13389c).

B. The Problem of Excess Currents

The nature of the unconstrained magnetic amplifier is such that current flows in any mesh during a portion of the cycle only. It is convenient to divide the half cycle of excitation frequency into the regions (Fig. MRI-13390):

(1) from 0 to A_1 when neither mesh conducts, $i_1 = i_2 = 0$.

(2) from A_1 to A_2 when only one mesh conducts, $i_1 = v/R_t, i_2 = 0$, with R_t as the total mesh resistance.

(3) from A_2 to π when both meshes conduct, $i_1 = v/r = i_2$, where r is the winding and rectifier forward resistance.

Load current, i, ($= i_1 - i_2$) flows only from A_1 to A_2, while from A_2 to π, very large currents, depending on the ratio of R_t to r, flow around the outside loop. Now the magnetic amplifier must be designed on the basis of the maximum dissipation in its windings (to a greater or lesser extent, depending on the duty cycle). We may define Relative Excess Current as the difference between the maximum current in the amplifier and the maximum current in the load, divided by the maximum load current. By currents here we mean rectified average currents.

C. Classification into Current and Voltage Type Amplifiers

For the purpose of discussing excess currents, it is appropriate to distinguish between two amplifier categories, which categories, of course have nothing to do with the previous classification. One of these may be called the "Current Amplifier" because the output current is (over the amplifying range) some constant times the input current, independent of the load or the excitation voltage. There is no excess current problem here. The mesh currents are held within bounds and although the circulating currents may be instantaneously large, their duration must be correspondingly small. The disadvantage of this type is its relatively low ampere-turns gain.

The second category of amplifier may be called the "Voltage Type Amplifier" because, over the amplifying range, it is the portion of the voltage cycle across the load, which is varied - from 0 to 100%. The output is voltage rather than current so that the latter is definitely a function of the applied voltage and resistance. There are no other bounds, as there are in the current amplifier, within which the rectified average mesh currents must stay. Excess currents, therefore, are a serious problem with this high-gain amplifier. When the high gain capabilities of the core are exploited, this is the type that results.

D. The Split-Feedback Circuit as a Solution to the Problem

The question is whether we can find a circuit that is a combination of the better parts of the voltage and current amplifier, so that we may have high gain with a check on the circulating currents. Such a circuit is described and analyzed in detail in this thesis. It is called the "Split-Feedback Push Pull Amplifier" (Fig. MRI-13397). Feedback windings are split and arranged in such a manner that when the two mesh currents are equal (i.e., when the circulating currents flow) there is no net feedback effect. However, when only one mesh current flows (load current), then there is a feedback effect.

As regards circulating currents it will be seen that at zero control current ($i_c = 0$), $I_1 = I_2 = (N_b/N)I_b$ —— 'i' capitalized means rectified average currents. Thereafter when control current flows, the circulating current decreases, as can quickly be seen as follows: The half-cycle may be divided into 3 regions — Region 1, when all cores are unsaturated and all currents are zero; Region 2, the load current region, where i_1 (say) $\neq 0$, and $i_2 = 0$ while Region 3 is the circulating current region where $i_1 = i_2$.

In Region 2 ... $i_1 N(1 - b) = i_{c1}N_c$ and $i_{c2}N_c = i_1 bN$

In Region 3 .... $i_{c2}N_c = i_2N$ and $i_1 = i_2$; $i_{c1} = i_{c2}$

Averaging the above results in:

$$I_{c1} = (N/N_c)(1 - b)I_{load} + (N/N_c) I_{circulating}$$

$$I_{c2} = b(N/N_c) I_{load} + (N/N_c) I_{circulating}$$

Subtracting, there results

$$I_{load} = (N_c/N) \frac{(I_{c1} - I_{c2})}{(1 - 2b)} = (N_c/N) \frac{I_c}{(1-2b)}$$

while adding, we have

$$I_{c1} + I_{c2} = 2I_b = (N/N_c) I_{load} + 2(N/N_c) I_{circulating}$$

Therefore, as I_L increases, $I_{circ.}$ must decrease since the left-hand side of the equation is a constant and when $2I_b = (N/N_c)I_L$ (maximum output for optimum biasing), $I_{circ.}$ is zero. Thus, in the useful range the circulating current is always bounded while the gain is that of a circuit with 100% feedback if $b = (N_f/N) = 1/2$. The maximum rectified average value of the circulating current is $(N_b/N) I_b$ which is exactly half the maximum (optimum biasing) output current.

A detailed mathematical analysis is presented in Section 3 but since this circuit possesses many of the properties of the push-pull current amplifier, the latter will first be analyzed. While it may be, of itself, only of moderate interest, its modes of operation are very similar to those of the more complicated split-feedback circuit and so, provides a good introduction to it.

II. The AC Push-Pull Current Amplifier

A. Analysis

The circuit is presented in Fig. MRI-13391a. Bias and control currents are taken as flowing in the same winding for convenience in analysis. Ideal B - H relationship is assumed (Fig. MRI-13391b).

"r" includes coil resistance, and any other mesh resistance not common (as is R) to both meshes.

For $R_c = R_b = 0$ we have, in the usual manner[1]:

$$\left.\begin{aligned} \Phi_{1a} + \Phi_{1b} &= \text{constant.} = \Phi_s + \Phi_{o1} \\ \Phi_{2a} + \Phi_{2b} &= \text{constant.} = \Phi_s + \Phi_{o2} \end{aligned}\right\} \quad (1)$$

We also have the mesh equations:

$$\left.\begin{aligned} v &= R_t i_1 - Ri_2 + N(\dot{\Phi}_{1a} - \dot{\Phi}_{1b}) = R_t i_1 - Ri_2 + 2N\dot{\Phi}_{1a} \\ v &= -Ri_1 + R_t i_2 + 2N\dot{\Phi}_{2a}, \quad \text{where } R_t = R + r \end{aligned}\right\} \quad (2)$$

The mmf equations for the cores are:

$$\left.\begin{aligned} H_{1a}l_m = h_{1a} &= i_{c1}N_c + i_1 N & H_{1b}l_m = h_{1b} &= i_{c1}N_c - i_1 N \\ h_{2a} &= i_{c2}N_c + i_2 N & h_{2b} &= i_{c2}N_c - i_2 N \end{aligned}\right\} \quad (3)$$

We may assume any mode of operation to begin with and find what it leads to. At random, then, all cores are unsaturated. Using (3), all currents are zero since all h's are zero. Using (2),

$$\dot{\Phi}_{1a} = -\dot{\Phi}_{1b} = \dot{\Phi}_{2a} = -\dot{\Phi}_{2b} = v/N$$

since the inductance is infinite.

At some time, say at $wt = A_1$, a core will saturate and with no loss in generality take it to be in mesh 1, either 1a or 1b. We may also assume operation until now in the positive half cycle with $\dot{\Phi}_{1a}$ positive:

(i) Core 1_a saturates	(ii) Core 1_b satruates
$\Phi_{1a} = \Phi_s$; $\Phi_{1b} = \Phi_{o1}$	$\Phi_{1b} = -\Phi_s$; $\Phi_{1a} = \Phi_{o1}$
$h_{1b} = 0$; $i_2 = i_{c2} = 0$	$h_{1a} = 0$; $i_2 = i_{c2} = 0$
$i_{c1}N_c = i_1 N = \lvert i_1 \rvert N = i_c N_c$	$i_{c1}N_c = -i_1 N = -\lvert i_1 \rvert N = i_c N_c$
$i_1 = v/R_t = i = (N_c/N)i_{c1}$	Same
$\dot{\Phi}_{2a} = -\dot{\Phi}_{2b} = (v/2NR_t)(1+R/R_t) = dv/2NR_t$	Same

This will continue until either one of No. 2 cores saturates or until the saturated core of Mesh 1 unsaturates. The latter case will be recognized as the limit case of the former. Following up with the two alternatives of core 2a or core 2b saturating at wt = A_2, less than π:

(iii) Core 2_a saturates

$\Phi_{2a} = \Phi_s$; $h_{2b} = 0$; $i = i_c = 0$

$i_1 = i_2 = v/r$; $i_{c2}N_c = i_2N = |i_2|N$

(iv) Core 2_b saturates

$\Phi_{2b} = -\Phi_s$; $h_{2a} = 0$; $i = i_c = 0$

$i_1 = i_2 = v/r$; $i_{c2}N_c = -i_2N = -|i_2|N$

This will go on until one or more cores unsaturates which they will all do simultaneously at wt = π since here all currents are zero.

In the negative half cycle we begin with all cores unsaturated until wt = $A_1 + \pi$, when one of No. 1 cores saturates first. This follows from our assumption that No. 1 fired first in the positive half cycle, since $\int_t^{t+T} d\Phi = 0$, so that there must be symmetrical operation.

(i) Core 1_b saturates

$\Phi_{1b} = \Phi_s$; $h_{1a} = 0$; $i_2 = i_{c2} = 0$

$i_1 = v/R_t = i$; $\dot{\Phi}_{2a} = \dot{\Phi}_{2b}(-1) = dv/2NR_t$

$i_{c1}N_c = -i_1N = |i_1|N = i_cN_c$

(ii) Core 1_a saturates

$\Phi_{1a} = -\Phi_s$; $h_{1b} = 0$; $i_2 = i_{c2} = 0$

same

$i_{c1}N_c = i_1N = -|i_1|N = i_cN_c$

The above continues until wt = $A_2 + \pi$, when:

(iii) Core 2_b saturates

$\Phi_{2b} = \Phi_s$; $h_{2a} = 0$; $i_1 = i_2 = v/r$

$i_{c2}N_c = -i_2N = |i_2|N$; $i = i_c = 0$

(iv) Core 2_a saturates

$\Phi_{2a} = -\Phi_s$; $h_{2b} = 0$; $i_1 = i_2 = v/r$

$i_{c2}N_c = i_2N = -|i_2|N$; $i = i_c = 0$

B. Modes of Operation

For a complete cycle we have the possible combinations: (1) - i and iii (2) - i and iv (3) - ii and iii (4) - ii and iv. Combinations 3 and 4 require that I_{c2} be positive and I_{c1} negative, so that for the polarities of E_b and E_c as in Fig. MRI-13391a, only the first two are possible. The corresponding waveforms are drawn in Figures MRI-13392a and MRI-13392b. For Combination 2, it should be noted that $K_2 = \Phi_{2a} + \Phi_{2b} = -\Phi_s + \Phi_{02}$.

To find over what ranges Combinations 1 and 2 are valid, consider the situation when $I_c = 0$, and $I_{c1} = I_{c2} = I_b$, which is a particular case of No. 1. As I_c increases, we have No. 1 with the relations:

$$I_{c1}N_c = I_1N; \qquad I_{c2}N_c = I_2N; \qquad I_cN_c = (I_{c1} - I_{c2})N_c = IN.$$

$$I_2 = (2/T)\int_{A_2}^{\pi} i_2 \frac{dt\omega}{\omega} = (I_m'/2)(1 + \cos A_2) \text{ where } I_m' = (2/\pi)\ V_m/r,$$

so that

$$\cos A_2 = 2\frac{N_c}{N}(I_b - \frac{I_c}{2})/I_m' - 1, \quad \text{where } I_b = 1/2\ (I_{c1} + I_{c2}).$$

Thus as I_c increases, cos A_2 becomes more negative, i.e., A_2 shifts to the right towards π. Simultaneously A_1 shifts to the left in order that I_1 remain equal to $(N_c/N) = (N_c/N)\ (I_b + I_c/2)$.

(1) Case I_x less than I_m ($I_x = 2(N_b/N)\ I_b$ which here = $2(N_c/N)I_b$.)

The limit of the above mode is reached either when $A_1 = 0$ or $A_2 = \pi$, whichever occurs first. At $A_2 = \pi$, $I_2 = I_{c2} = 0$ so that $I_b = I_c/2$ and $I = (N_c/N)I_c = 2(N_c/N)I_b = I_x$ (Fig. MRI-13393a). Obviously, in order for this to happen it is necessary that $I_m \geq I_x$, where $I_m = (2/\pi)V_m/R_t$. If $I_x > I_m$, $A_1 = 0$ must occur first. For the condition $I_m > I_x$, when I_c is increased beyond the point where $I_{c2} = 0$, I_{c2} goes negative and combination 2 applies. But now $\Delta I_1 = \Delta I_2 = (N_c/N)\Delta I_c/2$ algebrically, so that $\Delta I = 0$, i.e., the output saturates. This will continue until $A_1 = 0$.

As I_c is progressively increased, the cores of mesh 1 remain saturated throughout the entire cycle while the relation $\Delta I_2 = \Delta I_c/2(N_c/N)$ persists, so that ΔI_1 becomes proportional to area E in Fig. MRI-13393b while ΔI_2 becomes proportional to areas E + F. And now ΔI (to -F) = $-(I_m/I_m')\Delta I_2 = -(r/R_t)(N_c/N)\Delta I_c/2$. Thus I decreases linearly with I_c at a rate equal to $(N_c/N)1/2\ (r/2R_t)$ until $A_2 = 0$, when $I_1 = I_2 = I_m'$ and all cores are saturated over the entire cycle.

(2) Case I_m less than I_x

On the other hand, if $I_m < I_x$ then $A_1 = 0$ occurs before $A_2 = \pi$. When $A_1 = 0$, $I_1 = 1/2\ I_m(1 - \cos A_2) = (N_c/N)\ (I_b + 1/2\ I_c)$; $I_2 = (N_c/N)\ (I_b - I_c/2) = I_m'\ 1/2(1 + \cos A_2)$, resulting in $I_c(1 - r/2R_t) = I_mN/N_c - I_br/R_t$ at $A_1 = 0$. This value of I_c marks the limit of the main amplifying range and the maximum output for this range is therefore

$$(N_c/N)I_c = \frac{\frac{N_c}{N}\left(I_m\frac{N}{N_c} - I_b\frac{r}{R_t}\right)}{1 - r/2R_t} \approx I_m - (N_c/N)I_b(r/R_t).$$

Thereafter as I_c increases the cores of mesh 1 remain saturated while $\Delta I_2 = (N_c/N)\Delta I_c/2$, so that now the output increases with I_c at a rate equal to $(N_c/N)r/2R_t$ until $I = I_m$ (Fig. MRI-13393c, $\Delta I = H$). After that, as I_c increases, I decreases at the same slow rate until it is zero and $I_1 = I_2 = I_m'$.

When $I_x = I_m$, $A_1 = 0$ and $A_2 = \pi$ simultaneously, achieving maximum output within the amplifying range.

3. Rating of Cores

It should be noted that when $A_2 = \pi$ and $A_1 = 0$,

$$\int_0^{\pi/\omega} d\Phi_{2a} = \int_0^{\pi/\omega} (d)\ vdt/2N = (d)\ V_m/wN = (d)\Phi_m \leqslant 2\Phi_s.$$

For $R \gg r$, so that $\Phi_m \leqslant \Phi_s$, as compared to $\Phi_m \leqslant 2\Phi_s$ for the single mesh circuit.

C. Experimental Work

Fig. MRI-13394 compares the theoretical and experimental results for $I_x > I_m$ while Fig. MRI-13395 does the same for $I_m > I_x$. The minor differences can be ascribed to finite magnetizing current and to the difficulty in estimating correctly the rectifier forward effective resistance. Fig. MRI-13396a displays the waveforms for the case where $I_x > I_m$ near the point where the limit of the amplifying range is reached. The results should be compared to Fig. MRI-13392a containing the theoretical waveforms. To check for i_{c1} and i_{c2} of Fig. MRI-13392a, note that $i_b + i_c/2 = i_{c1}$; $i_b - i_c/2 = i_{c2}$.

The relatively minor difference in flux waveforms between theoretical and experimental is of course due to the finite values of R_c' and R_b which were taken as zero in the analysis.

Fig. MRI-13396b displays waveforms in the amplifying range. Again the minor deviations from theory in the flux waveforms are due to the finite values of control and bias circuit resistance.

Excess Currents

For practical purposes I_x would be made equal to I_m, so that the maximum output is obtained in the amplifying range, together with zero excess currents. At zero input, the quiescent (circulating) current is $I_m/2$, while the maximum output current is twice this value.

In the next section we will analyze the Split-Feedback circuit on the same basis of ideal B-H relationship.

III. Analysis of the Split Feedback Push-Pull Amplifier Based on Ideal B-H Characteristics

A. Analysis (Fig. MRI-13397)

The ideal B-H relation has been drawn in Fig. MRI-13391b. While this will result in infinite gain in the amplifying range, the analysis is nevertheless very useful in deducing the various modes of operation. In Section V an analysis will be carried out based on a more correct B-H relationship.

We proceed now in a manner very similar to Section II, with identical notation. As before, for

$$R_c = R_b = 0, \quad \dot{\Phi}_{1a} = \dot{\Phi}_{1b}; \quad \dot{\Phi}_{2a} = \dot{\Phi}_{2b} \tag{4}$$

$$v = R_t i_1 - Ri_2 - 2N\dot{\Phi}_{1a} = -Ri_1 + R_t i_2 - 2N\dot{\Phi}_{2a} \text{ (Fig. MRI-13397) (5) \& (6)}$$

$$H_{1a}{}^{l}{}_{m} = h_{1a} = -i_1 N - |i_1|N_f + |i_2|N_f - i_{c1}N_c \tag{7}$$

$$h_{1b} = -i_1 N + |i_1|N_f - |i_2|N_f + i_{c1}N_c \tag{8}$$

$$h_{2a} = -i_2 N + |i_1|N_f - |i_2|N_f - i_{c2}N_c \tag{9}$$

$$h_{2b} = -i_2 N - |i_1|N_f + |i_2|N_f + i_{c2}N_c \tag{10}$$

We shall now prove the following to be true:

(a) When $i_1 > 0$ and $i_{c1} > 0$, $h_{1a} < 0$, $\Phi_{1a} = -\Phi_s$, $h_{1b} = 0$
(b) " " " " " < 0, $h_{1b} < 0$, $\Phi_{1b} = -\Phi_s$, $h_{1a} = 0$
(c) " $i_1 < 0$ " " > 0, " > 0, $\Phi_{1b} = \Phi_s$, " "
(d) " " " " " < 0, $h_{1a} > 0$, $\Phi_{1a} = \Phi_s$, $h_{1b} = 0$
(e) " $i_2 > 0$ and $i_{c2} > 0$, $h_{2a} < 0$, $\Phi_{2a} = -\Phi_s$, $h_{2b} = 0$
(f) " " " and $i_{c2} < 0$, $h_{2b} < 0$, $\Phi_{2b} = -\Phi_s$, $h_{2a} = 0$
(g) " $i_2 < 0$ and $i_{c2} > 0$, $h_{2b} > 0$, $\Phi_{2b} = \Phi_s$, $h_{2a} = 0$
(h) " $i_2 < 0$ and $i_{c2} < 0$, $h_{2a} > 0$, $\Phi_{2a} = \Phi_s$, $h_{2b} = 0$
(i) " $i_1 = 0$, $|i_2|N_f = i_{c1}N_c$, and $h_{1a} = h_{1b} = 0$
(j) " $i_2 = 0$, $|i_1|N_f = i_{c2}N_c$, and $h_{2a} = h_{2b} = 0$
(k) " $i_1 = i_2 = i_{c1} = i_{c2} = 0$, $h_{1a} = h_{1b} = h_{2a} = h_{2b} = 0$.

The above is true providing the parameters of the circuit are such that both cores of any mesh cannot saturate simultaneously. (i) is proven by adding (7) and (8) giving $h_{1a} + h_{1b} = 0$, and then subtracting (7) from (8), giving $h_{1b} - h_{1a} = 2i_{c1}N_c - 2|i_2|N_f$. Since either h_{1b} or h_{1a} must be zero, both must be zero in this case and therefore $i_{c1}N_c = |i_2|N_f$. "(j)" is similarly proven from (9) and (10), while (k) follows from (i) and (j).

Statement (b) is proven as follows:

(7) + (8) yield $h_{1a} + h_{1b} = -2i_1N$

(7) - (8) yield $h_{1a} - h_{1b} = -2|i_1|N_f + 2|i_2|N_f + 2|i_{c1}|N_c$

Now, if $h_{1b} = 0$, then

$$h_{1a} = -2i_1N = -2|i_1|N_f + 2|i_2|N_f + 2|i_{c1}|N_c$$

and

$$-i_1N + |i_1|N_f = |i_2|N_f + |i_{c1}|N_c.$$

The left side is negative because $i_1 > 0$ and $N > N_f$ which doesn't agree with the fact that the right side is positive. Therefore $h_{1b} \neq 0$. If $h_{1a} = 0$, then $-i_1N(1 + b) = -|i_2|N_f = -|i_{c1}|N_c$ where $b = N_f/N$, and there is no such contradiction. Since $h_{1a} + h_{1b}$ is negative, from (7) + (8), one of them must be negative, and the other zero, and the latter must be h_{1a}.

Statements (d), (f) and (h) are proven in the same manner.

The proof of statement (a) runs as follows:

$$h_{1a} + h_{1b} = -2i_1N$$

therefore one must be negative, the other zero.

$$h_{1b} - h_{1a} = 2(|i_1|N_f + i_{c1}N_c - |i_2|N_f)$$

which is positive if

$$|i_1|N_f + i_{c1}N_c > |i_2|N_f.$$

If this is always true, then, following the reasoning in proving (b), $h_{1a} < 0$, $h_{1b} = 0$. We must therefore prove that $|i_1|N_f + i_{c1}N_c > |i_2|N_f$.

If both i_1 and $i_2 \neq 0$, $i_1 = i_2$ by considering equations (5) and (6) and noting that if $i_1 \neq 0$, $\dot{\Phi}_{1a} = 0$, because of infinite inductance. If $i_2 \neq 0$, $\dot{\Phi}_{2a} = 0$, and therefore if $i_1 \neq 0$, $i_2 \neq 0$, $i_1 = i_2$ from (5) and (6) and the relation $|i_1|N_f + i_{c1}N_c > |i_2|N_f$ is certainly true. If $i_1 \neq 0$, $i_2 = 0$, it is certainly true. The only alternative left is that $i_1 = 0$, $i_2 \neq 0$, and it is not tenable because it contradicts the assumption under (a), that $i_1 > 0$.

Statements (c), (e) and (g) are similarly proven.

We may conveniently begin at that part of the cycle (positive half when all the cores are unsaturated with all h's zero, so that all i's are zero and $\dot{\Phi}_{1a} = \dot{\Phi}_{1b} = \dot{\Phi}_{2a} = \dot{\Phi}_{2b} = -V_m \sin wt/2N$. At some time, say at $wt = A_1$, a core will saturate and with no loss in generality take it to be in mesh 1. The procedure is now the same as in the current amplifier.

(i) 1_a saturated

$\Phi_{1a} = -\Phi_s$; $\Phi_{1b} = \Phi_{o1}$; $h_{1b} = i_2 = 0$

$i_{c1}N_c = i_1N(1-b) = |i|N(1-b) = |i_1|N(1-b)$

$i_{c2}N_c = |i_1|bN$; $i_1 = V_m \sin wt/R_t$

$\dot{\Phi}_{2a} = \dot{\Phi}_{2b} = -vd/2N$

(ii) 1_b saturated

$\Phi_{1b} = -\Phi_s$; $\Phi_{1a} = \Phi_{o1}$; $h_{1a} = i_2 = 0$

$i_{c1}N_c = -|i_1|N(1+b) = -|i|N(1+b)$

$i_{c2}N_c = |i_1|bN$; $i_1 = V_m \sin wt/r_t$

$\dot{\Phi}_{2a} = \dot{\Phi}_{2b} = -vd/2N$

At $wt = A_2$, one of mesh 2 cores will saturate, 2a or 2b:

(iii) 2_a saturated

$\Phi_{2a} = -\Phi_s$; $\Phi_{2b} = \Phi_{o2}$; $i = h_{2b} = 0$

$i_{c2}N_c = |i_2|N$; $i_1 = i_2 = v/R_t$

(iv) 2_b saturated

$\Phi_{2b} = -\Phi_s$; $\Phi_{2a} = \Phi_{o2}$; $h_{2a} = i = 0$

$i_{c2}N_c = -|i_2|N$; $i_1 = i_2 = v/R_t$

Unsaturation occurs simultaneously for all cores at $wt = \pi$, since at this instant all i's are zero. From π until $\pi + A_1$, then, all i's are zero and $\dot{\Phi}_{1a} = \dot{\Phi}_{1b} = \dot{\Phi}_{2a} = \dot{\Phi}_{2b} = -V_m \sin wt/2N$. At $wt = \pi + A_1$ one of No. 1 cores will saturate, 1_b if 1_a has saturated in the first half cycle and vice versa:

(i) 1_B saturated

$\Phi_{1b} = \Phi_s$; $\Phi_{1a} = \Phi_{o1}$; $h_{1a} = i_2 = 0$

$i_{c2}N_c = |i_1|N_f$; $i_1 = v/R_t = i$

$i_{c1}N_c = |i_1|N(1-b)$

(ii) 1_A saturated

$\Phi_{1a} = \Phi_s$; $\Phi_{1b} = \Phi_{o1}$; $h_{1b} = i_2 = 0$

Same

$i_{c1}N_c = -|i_1|N(1+b)$

At wt = $A_2 + \pi$, one of No. 2 cores will saturate:

(iii) 2_B saturated

$\Phi_{2b} = \Phi_s$; $\Phi_{2a} = \Phi_{o2}$; $i_1 = i_2 = v/r$

$h_{2a} = 0$; $i_{c2}N_c = |i_2|N = i_{c1}N_c$

(iv) 2_A saturated

$\Phi_{2a} = \Phi_s$; $\Phi_{2b} = \Phi_{o2}$; $i_1 = i_2 = v/r$

$h_{2b} = 0$; $i_{c1}N_c = -|i_1|N = i_{c2}N_c$

B. Modes of Operation

As before the following combinations are possible:
(1) - i and iii (2) - i and iv (3) - ii and iii (4) - ii and iv
Here, as in the current amplifier, (3) and (4) may be discarded because of the assumed polarities of E_b and E_c. Thus (3) and (4) result in the waveforms of i_{c1} and i_{c2} as in Fig. MRI-13399a and MRI-13399b with I_{c1} (true mean), negative, contrary to the polarities of E_b and E_c. For combination (1), the waveforms are drawn in Fig. MRI-13399c, while the relations between the various currents may now be worked out:

$$\bar{I}_{c1} = (2/T)\left(\int_{A_1/\omega}^{A_2/\omega} i_{c1}\,dt + \int_{A_2/\omega}^{\pi/\omega} i_{c1}\,dt\right) = (2/T)\left[\left(\frac{N}{N_c}\right)(1-b)\int_{A_1/\omega}^{A_2/\omega}(v/R_t)\,dt + \frac{N}{N_c}\int_{A_2/\omega}^{\pi/\omega} v/r\,dt\right]$$

$$\bar{I}_{c2} = (2/T)\left[(bN/N_c)\int_{A_1/\omega}^{A_2/\omega} v/R_t\,dt + (N/N_c)\int_{A_1/\omega}^{A_2/\omega}(v/r)\,dt\right]$$

Therefore

$$\bar{I}_c = \bar{I}_{c1} - \bar{I}_{c2} = (2/T)(1-2b)(N/N_c)\int_{A_1/\omega}^{A_2/\omega}(v/R_t)\,dt = (1-2b)\,I(N/N_c)$$

so that

$$\text{Gain} = (I/I_c) = (1/1-2b)(N/N_c)$$

For 100% feedback, $b = N_f/N = 1/2$ with theoretically infinite gain.

We also have $I_{c1}+I_{c2} = \text{constant} = (2/T)(N/N_c)\left[\left(\int_{A_1/\omega}^{A_2/\omega} i_1\,dt + \int_{A_2/\omega}^{\pi/\omega} i_1\,dt\right)\right]$

Therefore $2I_b = (N/N_c)\left[(I + (I_m/(2-d))(1 + \cos A_2)\right]$

or

$$2I_b(N_c/N) = I_x = I + (1 + \cos A_2)\,(I_m/2-d) \qquad (11)$$

This equation is very useful. We know that at $I_c = 0$,

$$I_{c1} = (2/T)(N/N_c) \int_{A_o/\omega}^{\pi/\omega} v/r \, dt = I_1(N/N_c) = I_2(N/N_c) = I_b$$

so that with zero input, $I_1 = I_2 = I_b(N_c/N) = I_x/2$, and $\cos A_o = 2\frac{N_c}{N}\frac{I_b}{I_m} - I$ (setting $I = 0$ and $A_2 = A_o$ in Equation (11)).

Wehn I_c is increased, we have Mode (1) with high gain, until some limiting point is reached. Just when this point is reached depends upon the relative values of $I_x = 2I_b(N_c/N)$ and $I_m = (2/\pi)(V_m/R_t)$. This can be seen by examining Equation (11) and the following:

$$I = (2/T) \int_{A_1/\omega}^{A_2/\omega} \frac{V_m \sin \omega t}{R_t} dt, \text{ so that } \cos A_1 = \frac{I_x(2-d) + Id}{I_m} - 1 \quad (12)$$

As I increases, A_2 must increase (shift to the right) in order that the right-hand side of Equation (11) remain constanr. Simultaneously, A_1 must decrease (shift to the left) from Equation (12). The interval, $A_2 - A_1$, in which the useful load current flows, increases until either $A_1 = 0$ or $A_2 = \pi$. If the latter occurs first, $I_x = I$ (from Equation (11)), so that obviously $I_m > I_x$ to make this possible. If $A_1 = 0$ occurs first, then $I = (I/2)(\cos A_1 - \cos A_2) = (I_m/2)(1 - \cos A_2)$ while Equation (11) becomes $(I_x/I_m) = (1/2(2-d))(4-d+d \cos A_2)$. Now $d = 1 + R/R_t$ so that $1 \leq d \leq 2$. It can be seen that for 'd' in this range, $(I_x/I_m) \geq 1$, so that when this is true, $A_1 = 0$ occurs first. For this case the value of I at this point is obtained by setting $A_1 = 0$ in out equations, resulting in

$$I = \frac{2I_m - I_x(r/R_t)}{2 - (r/R_t)}$$

If $I_x = I_m$, $A_1 = 0$, and $A_2 = \pi$ simultaneously, and Mode (1) is over at $I = I_m$. This is the best practical condition, for the maximum output is gotten in the amplfying range.

If $I_m > I_x$, Mode (1) is over when $I = I_x$, $A_2 = \pi$, $A_1 \neq 0$. If $I_m < I_x$, Mode (1) is over when $A_1 = 0$, $I = (2/d)I_m - (2-d/d)I_x$.

Another way of seeing this is to examine the flux waveforms of Fig. MRI-13399c. At the interval, $A_2 - A_1$, increases (A_1 shifting to the left and A_2 to the right) there is less time for Φ_{1a} and Φ_{1b} to depart from saturation, i.e., Φ_{o1} increases until at $A_1 = 0$, the cores of No. 1 mesh remain saturated throughout the entire cycle (Fig. MRI-13402c). At the same time there is more time for Φ_{2a} and Φ_{2b} to change, until at $A_2 = \pi$

or sooner (depending upon the relative values of Φ_m and Φ_s), these cores remain unsaturated throughout the entire cycle. If Φ_m is too large, complete unsaturation will never occur. As to whether the No. 1 cores stay saturated before or after the No. 2 cores become completely unsaturated, this depends entirely on the ratio of I_x to I_m.

Quantitively, by integrating Φ_1 from 0 to A_1,

$$\Phi_{o1} = \Phi_s - \Phi_m \frac{(1 - \cos A_1)}{2}, \text{ and integrating from } A_1 \text{ to } A_2,$$

$$\Phi_{o1} - \Phi_{o2} = (I/I_m)\,\Phi_m d, \text{ and since } 2I/I_m = \cos A_1 - \cos A_2,$$

we have

$$\Phi_{o1} = \Phi_s - (\Phi_m/2)\left(2 - \frac{I_x(2-d) + Id}{I_m}\right)$$

$$\Phi_{o2} = \Phi_s - (\Phi_m/2)\left(2 - \frac{I_x(2-d) - Id}{I_m}\right)$$

As I increases, Φ_{o2} decreases while Φ_{o1} increases.

(1). Cases $I_x > I_m$

What happens when I_c is increases beyond the limit point of Mode (1)? If $I_x > I_m$, the cores of No. 1 remain saturated at all times and from zero to A_2, $i_1 = i = v/R_t$ and $\dot{\Phi}_{2a} = \dot{\Phi}_{2b} = (-vd/2N)$. Since $h_{2a} = h_{2b} = 0$, $i_{c2}N_c = |i_1|bN$, and i_{c1} = constant = I_{c1}. From A_2 to π, $i_1 = i_2 = v/r$, $h_{2b} = 0$, so that $i_2 N = i_{c2} N_c$. Therefore

$$(T/2)I_{c2} = bN/N_c \int_0^{A_2/\omega} v/R_t \, dt + N/N_c \int_{A_2/\omega}^{\pi/\omega} v/r \, dt.$$

$$I_{c2} = b(N/N_c)(I_m/2)(1 - \cos A_2) + (N/N_c)(I_m/2)(1 + \cos A_2).$$

Rearranging:

$$\cos A_2 = \frac{2\,\frac{N_c}{N}\,\frac{I_{c2}}{I_m} - \left(b + \frac{R_t}{r}\right)}{\frac{R_t}{r} - b}$$

$$I = I_m \frac{\left(\frac{R_t}{r} - \frac{N_c}{N}\,\frac{I_{c2}}{I_m}\right)}{\frac{R_t}{r} - b} \quad \text{and } \Delta I \doteq (r/R_t)\,(N_c/N)\,\Delta I_c/2, \text{ i.e., low gain.}$$

With increase of I_c, I_{c2} decreases, so that A_2 increases, shifting to the right and I increases until at $A_2 = \pi$, $I = I_m$. The value of I_{c2} at $A_2 = \pi$, is $I_{c2} = (bNI_m)/N_c = I_b - I_c/2$. If I_c is increases beyond this value, A_2 decreases, shifting back to the left but now from zero to A_2...

$$i_1 = i = v/R_t \; ; \; \dot{\Phi}_{2a} = \dot{\Phi}_{2b} = -vd/2N; \; h_{2a} = h_{2b} = 0;$$

$i_{c2}N_c = |i_1|bN$, all as before. However, from A_2 to π, $h_{2a} = 0$ (and not h_{2b} as before), i.e., Core 2_B saturates where 2_A had previously saturated, so that from Equation (9), $i_{c2}N_c = -|i_2|N$. This can be understood by considering that at $A_2 = \pi$, the net mmf of No. 2 cores is zero, i.e., due to control-bias ampere turns we have $N_cI_{c2} = bNI_m$ while due to NI_2 there is zero (at $A_2 = \pi$, I_2 is zero); and due to I_1 we have $-bNI_m$ (at $A_2 = \pi$, $I_1 = I_m$). That is why the cores remain unsaturated if $\Phi_m d \leq 2\Phi_s$. When I_c is increased, the net mmf changes sign and the two cores shift accordingly in the operation cycle. Integrating, we get:

$$I_{c2} = (N/2N_c)\left[(b - R_t/r - \cos A_2(b + R_t/r)\right], \text{ so that ....}$$

$$\cos A_2 = \left[b - R_t/r - 2N_cI_{c2}/(NI_m)\right]/(b + R_t/r).$$

From this expression for cos A_2, it is seen A_2 shifts to the left with increasing I_c (decrease of I_{c2}). Also:

$$I = (I_m/2)(1 - \cos A_2) = I_m(R_t/r + N_cI_{c2}/NI_m)/(b + R_t/r)$$

and $\Delta I \doteq -rN_c\Delta I_c/(R_tN_2)$. The limit ($I = 0$; $A_2 = 0$) is reached when $(R_t/r) = -N_cI_{c2}/NI_m$, by setting cos $A_2 = 1$ in the above expression.

(2). Case: $I_m > I_x$

On the other hand, when $I_m > I_x$, if I_c is increased beyond the saturation point (which we have found to be at $I = I_x$), then combination (2) applied. The waveforms applicable are presented in Fig. MRI-13399d.

The relations between the various currents for this mode are:

$$(T/2)\, I_{c1} = (1 - b)\, N/N_c \int_{A_1/\omega}^{A_2/\omega} i_1 dt + N/N_c \int_{A_2/\omega}^{\pi/\omega} i_1 dt.$$

$$(T/2)\, I_{c2} = b\, N/N_c \int_{A_1/\omega}^{A_2/\omega} i_1\, dt - N/N_c \int_{A_2/\omega}^{\pi/\omega} i_1\, dt.$$

Adding: $$(T/2)(I_{c1} + I_{c2}) = (N/N_c) \int_{A_1/\omega}^{A_2/\omega} i_1 dt = T/2(NI)/N_c$$

so that: $$I = (N_c/N)\,(I_{c1} + I_{c2}) = 2N_c I_b/N = I_x.$$

Therefore I remains constant throughout this mode. Also:

$$I_{c1} - I_{c2} = (2/T)\left[N(1-2b)/N_c \int_{A_1/\omega}^{A_2/\omega} i_1 dt + 2N/N_c \int_{A_2/\omega}^{\pi/\omega} i_1 dt\right] = I_c$$

i.e., I_c = Input causing saturation $+\left[I_m N/(2-d)N_c\right](1+\cos A_2) = I_s$ + the balance. This equation determines A_2. Since

$$I = I_1 - I_2,\quad \Delta I = \Delta I_1 - \Delta I_2,$$

and in this range $\Delta I = 0$, therefore $\Delta I_1 = \Delta I_2$. Also

$$I_1 = I + (2/T) \int_{A_2/\omega}^{\pi/\omega} V_m/r \sin wt\, dt = I + I_2.$$

$$\Delta I_1 = (I_m'/2)(1 + \cos A_2),\ \text{resulting in}\ (I_c - I_s)/2 = \Delta I_c/2 = (N/N_c)\Delta I_1.$$

It seems therefore that in this range both meshes behave as current amplifiers with unity ampere-turns gain with respect to changes in control current.

The above will continue until $A_1 = 0$. At this point:

$$I = I_x = (I_m/2)(1 - \cos A_2);\ I_c = I_s + I_m' N/N_c(1+\cos A_2),$$

therefore

$$I_c - I_s = 2(N/N_c)(R_t/r)(I_m - I_x).$$

Henceforth A_1 remains at zero, while A_2 decreases (shifts to the left) and the operation is similar as for the case $I_x > I_m$.

When separate windings are used for contril and bias currents, then following the procedure in the current amplifier analysis,

$$I_x' = 2\,\frac{N_b}{N}\,I_b,$$

and for $N_c I_{c1}$ and $N_c I_{c2}$,

there should be substituted, respectively,

$$N_b I_b + N_c I_c/2 \quad \text{and} \quad N_b I_b - N_c I_c/2.$$

3. Summary for Cases (1) and (2)

(I) $I_m \geqslant I_x$

(1) $0 \leqslant I_c \leqslant I_{s1}$

(where $I_{s1} = 0+$) Amplifying range. Limit of range is reached when $I = I_x = 2I_bN_b/N$, at which point $I_1 = I_x$, $I_2 = 0$. At $I_c = 0-$, $I_1 = I_2 = I_x/2$, which is the maximum circulating current.

(2) $I_{s1} \leqslant I_c \leqslant I_{s2}$

(where $I_{s2} = I_{s1} + 2(R_t/r)(N/N_c)(I_m - I_x)$; $I = I_x$; $I_1 = I_x + (1/2)(N_c/N)(I_c - I_{s1})$; $I_2 = (1/2)(N_c/N)(I_c - I_{s1})$.

(3) $I_{s2} \leqslant I_c \leqslant I_{s3}$

(where $I_{s3} = I_{s1} + (2/N_c)(R_t/r)NI_m + N_bI_b$).

$$I = \frac{I_m}{b + \frac{R_t}{r}} \left[\frac{R_t}{r} + \frac{N_bI_b - N_cI_c/2}{NI_m} \right] \text{ so that } \Delta I = \frac{r}{R_tN} N_c \Delta \frac{I_c}{2}$$

$$\Delta I_2 = (I_m'/I_m) \left[1/(b + R_t/r) \right] N_c/N \, \Delta I_c/2 = \frac{N_c \Delta I_c}{N \; 2}$$

(4) $I_c \geqslant I_{s3}$; $I = 0$; $I_1 = I_2 = I_m'$

(II) $I_m \leqslant I_x$

(1) $0 \leqslant I_c \leqslant I_{s4}$

(I_{s4} analagous to I_{s1}). Amplifying range. Limit of range is reached when $I = (2I_m - I_x \, r/R_t)/(2 - r/R_t)$ and $I_2 = \frac{I_m'(-b + N_bI_b/NI_m)}{(R_t/r - b)}$

(2) $I_{s2} \leqslant Ic \leqslant I_{s5}$

(where $I_{s5} = I_{s4} + (N/N_c)(I_x - 2bI_m)$.

$$I = \frac{I_m \left(\frac{R_t}{r} - \frac{N_cI_{c2}}{NI_m} \right)}{\frac{R_t}{r} - b} \; ; \quad \Delta I = \frac{rN_c \, \Delta I_c}{R_tN \; 2}; \quad \Delta I_2 = \frac{\frac{-I_m'}{I_m} \frac{N_c}{N} \frac{I_c}{2}}{\frac{R_t}{r} - b} = -N_c \Delta I_c/(2N)$$

Limit is reached when $I = I_m$.

(3) $I_{s5} \leq I_c \leq I_{s6}$

(where $I_{s6} = I_{s4} + (2/N_c)(N_b I_b + N I'_m)$

$$\Delta I = \frac{-N_c \Delta I_c}{N \quad 2} \Big/ \left(b + \frac{R_t}{r}\right) \doteq \frac{-rN_c \Delta I_c}{R_t N \quad 2}\,; \quad \Delta I_2 = \frac{I'_m N_c \Delta I_c/2}{b + R_t/r} \doteq \frac{N_c}{N} \Delta \frac{I_c}{2}.$$

(4) $I_c \geq I_{s6}$ $\quad I = 0;\ I_1 = I_2 = I'_m.$

O. Experimental Work

Fig. MRI-13400a, MRI-13400b and MRI-13400c compare theoretical and experimental curves for $I_m > I_x$ and $I_m < I_x$. As expected, there is disagreement over the amplifying range, but the agreement is good everywhere else, where the theory does claim accuracy. Fig. MRI-13401a presents the current waveforms of the circuit in its amplifying range. These compare very well with the predicted waveforms of Fig. MRI-13399c.

Fig. MRI-13401b waveforms are for the case $I_m > I_x$, in the saturated range. These should be compared with the theoretical waveforms of Fig. MRI-13399d. A departure from theory is the fact that from A_2 to π, $i_1 > i_2$, so that $i \neq 0$ in this region. This difference is probably due to the effect of finite impedances in the control and bias circuits. If one does take these into account, the algebra becomes quite complicated, but one finally emerges with the following (in the saturated region): $i_1 - i_2 = G + bN^2 v + H$, where G and H are constants gotten from solving the following pair of simultaneous equations:

$$(i_1 - i_2)\,(R_t + R + (N^2/N_c^2)R_b) + 2bNr(i_1 + i_2) = 2E_b N/N_c + 4bNv$$

$$(i_1 - i_2)2bN - (i_1 + i_2)\left(N + \frac{N_c^2 r}{N(2R_c + R_b)}\right) = -2v\frac{N_c}{N} - \frac{2N_c E_c}{R_b + 2R_c}$$

Thus $(i_1 - i_2)$ is a function of 'v' in this range which is in accordance with the waveform observed (Fig. MRI-13401b.

Fig. MRI-13401c presents waveforms of the output current 'i' as it changes from the positive saturation region (1) $(I_m > I_x)$, to the exact point of saturation (2) and in the amplification range (3), to corresponding negative values.

The waveforms of Fig. MRI-13402a are for the case $I_m < I_x$ at the point where the amplification range is ending, i.e., $A_1 = 0$. Fig. MRI-13401c(2) may be contrasted to Fig. MRI-13402a (1). Fig. MRI-13402b continues with the circuit of Fig. MRI-13402a with input increased past the point where $A_2 = \pi$, i.e., A_2 is now decreasing. The effect of finite resistance in the control and bias windings is again noted.

Fig. MRI-13402c(1) exhibits the B-H loop at zero output (similar for all the cores), while '2' and '3' are the loops of Cores 1 and 2 (one from each mesh) when I is large, almost at its maximum vlaue ($I_x = I_m$). It is seen that Core 2 saturates over a very small portion of the cycle, as $A_2 \doteq \pi$, while Core 1 is saturated almost over the entire cycle, as $A_1 \doteq 0$. Figures MRI-13402c(4) and MRI-13402c(5) are loops for the same cores, as I_c is further increased, so that Core 2 saturates in the other direction as predicted, while Core 1 remains saturated almost throughout the entire cycle. In this particular case, this change in sign of saturation of Core 2 occurred before A_1 went to zero, because Φ_m/Φ_s was 46.5/38.0, so that it was impossible for Core 1 to remain unsaturated throughout the entire cycle.

Summarizing, this section has dealt with the modes of operation of the Split-Feedback Push-Pull Amplifier, exhibiting clearly both analytically and experimentally its combination of desirable Voltage type amplifier and Current amplifier properties.

Because of the ideal B-H characteristic assumed for analysis, it was not possible to predict analytically and gain of the circuit in its amplifying (or Voltage type amplifier) range. To do this we must use a more accurate representation of the B-H relationship. We should like to use as close an approximation to the actual loop as would still permit relatively simple mathematics.

In the following three Sections such a representation is used to analyze firstly the Series circuit with 100% feedback (Section 4), secondly, the Push-Pull Split Feedback circuit with 100% feedback (Section 5) and finally the Push-Pull Voltage Doubler circuit in Section 6.

IV. Analysis of Series Circuit With 100% Feedback on Basis of Simplified B-H Hysteresis Loop

A. Analysis

The circuit is presented in Fig. MRI-13403a. $N_f = N$; $R_t = R + r$. If $R_c = 0$, $\Phi_1 - \Phi_2 =$ a constant. Also:

$$h_1 = N(i + |i|) + N_c i_c. \qquad h_2 = N(i - |i|) - N_c i_c$$

$$\text{If } i > 0, \quad h_1 = 2Ni + N_c i_c \text{ and } h_2 = -N_c i_c \tag{13}$$

$$\text{If } i < 0, \quad h_1 = N_c i_c \text{ and } h_2 = 2Ni - N_c i_c \tag{14}$$

On the basis of an ideal B-H relation of Fig. MRI-13403b, we have the waveforms drawn in Fig. MRI-13403c[2]. But the flux excursions as a function of 'h' are as in Fig. MRI-13404a and this B-H relationship should be used to find the actual gain.

We may begin with the positive conduction period - K in Fig. MRI-13403c. Here $\Phi_1 = \Phi_s$, $\Phi_2 = -\Phi_o$. Since (13) applies, $h_2 = h_o = -N_c i_c$ so that $i_c = -h_o/N_c$ and $i = v/R_t$. To facilitate the analysis considerably, Fig. MRI-13404a is appreximated by Fig. MRI-13404b. The following analysis is therefore restricted to materials where such an approximation is justifiable.

When $h_1 = -h_x$, Φ_1 begins to unsaturate and this will happen when $h_1 = 2Ni + N_c i_c = 2Ni - h_o = -h_x$, i.e., $(h_o - h_x)/2N = V_m \sin wt/R_t$, which for the sensitive materials considered is very nearly at $wt = \pi$. Note that h_x, h_o, etc. are all positive.

From π to $\pi + A_1$, both cores are unsaturated with Φ_1 and Φ_2 travelling along paths L-M-N. In this interval, $\dot{\Phi}_1 = \dot{\Phi}_2 = v/2N$ essentially and since $|h_o| > |h_x|$, 'i' is positive at the start of this interval. The transition from $i_1 +$ to $i_1 -$ cannot take place instantly as this would cause $\dot{\Phi}$ to become positive, so that it must actually do so at a finite rate until the instantaneous voltage is sufficiently negative to cause $\dot{\Phi}$ to continue to be negative. Now the path L_2-M_2-N_2 for Core 2 is difficulat to determine and is a function of several variables, so the approximation has been made that it is flat until or beyond $h_2 = h_x$. In such a case $h_1 = -h_2$ almost instantly with 'i' changing sign, so that condition (2) applies. Here $h_1 = N_c i_c$. In this interval

$$\int_{\Phi_s}^{\Phi_1} d\Phi_1 = V_m/2N \int_{\pi/\omega}^{t/\omega} \sin wt \, dt.$$

$$\Phi_1 = \Phi_s - (\Phi_m/2)(1 + \cos wt) \quad \text{where } \Phi_m = V_m/wN.$$

$$h_1 = N_c i_c = -h_x - (h_m/2)(1 + \cos wt).$$

This continues until $\pi + A_1$, when $\Phi_2 = \Phi_s$ and from then until 2π, $i = v/R_t$, $\Phi_2 = -\Phi_s$ and $h_1 = -|h_o| = N_c i_c$.

$$I = (2/T) \int_{A_1/\omega}^{\pi/\omega} V_m \sin \omega t / R_t \, dt = (I_m/2)(I + \cos A_1).$$

$$\Phi_o' = \Phi_s - \Phi_m(1 - \cos A_1)/2 \quad (I/I_m) + (\Phi_s - \Phi_o)/\Phi_m = 1.$$

$$1/2 \, N_c I_c = \int_{\pi+A_1}^{2\pi} |h_o| \, d\omega t/\omega + \int_{\pi}^{\pi+A_1} |h_x| + (h_m/2)(1+\cos \omega t) \, d\omega t/\omega.$$

$$N_c I_c = 1/\pi \left[|h_o|(\pi - A_1) + A_1(h_x + h_m/2) - h_m/2 \sin A_1 \right].$$

Since there is actually no abrupt break at I_1 (Fig. MRI-13404b) as was assumed, it is better to find $\Delta N_c I_c$, and

$$\Delta N_c I_c = N_c I_c - h_x = 1/\pi \left[(\pi - A_1)(h_o - h_x) + A_1 h_m/2 - (h_m/2) \sin A_1 \right]$$

If we let $k = \left| \Delta \frac{\Phi}{\Phi_s} / \Delta h \right|$, then:

$$N_c I_c = 1/k\pi \left[(\pi - A_1)\left(\frac{\Phi_s - \Phi_o}{\Phi_s}\right) + (A_1 - \sin A_1)\frac{\Phi_m}{2\Phi_s} \right]$$ where A_1, Φ_o and I/I_m are related to each other as previously noted:

$$\frac{\Phi_s - \Phi_o}{\Phi_s} = \left(1 - \frac{I}{I_m}\right)\left(\frac{\Phi_m}{\Phi_s}\right) \quad \text{and} \quad \cos A_1 = 2\frac{I}{I_m} - 1.$$

Average Gain

When $I = I_m$, $\Phi_s = \Phi_o$, $A_1 = 0$, $\Delta h = 0$. When $I = 0$, $A_1 = \pi$, and therefore $\Delta N_c I_c = \Phi_m / 2k\Phi_s$. Thus Average Output/Ampere-Turns Input = $I_m 2k\Phi_s/\Phi_m$. Thus to find the relationship between $N_c I_c$ and I/I_m, assume values of I/I_m, and substitute in the expression for $N_c I_c$.

B. Experimental Work

To check on the accuracy of the above analysis, it is essential, of course, that the correct control magnetization curve be used. This is a study in itself and regrettably there wasn't the time available for such a study. The experimental transfer curves for the half-wave constrained, self-saturing circuit were used. On this basis, of course, differences between the analysis and the experimental results may be ascribed either to the analysis or the use of an incorrect control magnetization curve. In short, in such a case, only very partial conclusions may be drawn.

For the half-wave constrained, self-saturating circuit:[3] $(\Phi_o/\Phi_s) = 1 - 2\,\Phi_m/\Phi_s(1 - 2\,I/I_m)$. Thus Φ_o/Φ_s may be related to I/I_m, and experimentally to N_cI_c. Fig. MRI-13406 presents curves for Φ_o/Φ_s as a function of 'h' for the self-saturating circuit under different conditions. All calculations are contained in the Appendix. For Curve 1, 1 cores was used with 2 rectifier descs (Radio Receptor D1H1), and $\Phi_m/\Phi_s = 0.97$. For Curve 2, 1 cores with 4 discs and $\Phi_m/\Phi_s = 1.0$, while for Curve 3, 2 cores in series were used with 4 rectifier discs and $\Phi_m/\Phi_s = 1.0$. Taking the average slopes of these curves over their amplifying range, the results are k = 0.68; 0.97 and 0.64 per Ampere-Turn.

Fig. MRI-13407 presents the experimental results obtained with the Series 100% Feedback Amplifier. In one case one rectifier disc was used per bridge arm; in the second case two were used. On the basis of our analysis, for the three values of k, for the particular parameter values used in the series circuit, the average slopes should be: 112, 160, 105 as compared to the experimental values of 70 to 80 (depending over what range the averaging is done).

Waveforms are presented in Fig. MRI-13405 and should be compared with Figures MRI-13403c and MRI-13404c.

Discussion

The differences between theoretical and experimental results may be ascribed to the following:

1. The approximations made in the analysis in neglecting control circuit resistance. This can be corrected - we can improve the analysis by taking it into account, but the result is very involved indeed. For example, to find the currents in the unsaturated region, we get the following expression for h_1:

$$h_1\left(\frac{4N^2N_c}{m^2R_t}\right) + h_1\left(\frac{2N_c}{m} + \frac{4R_cN^2}{N_cmR_t}\right) + \frac{h_1R_c}{N_c} = E_c + \frac{2NN_c\Phi}{mR_t}$$

where $m = dh/d\Phi$. Again time did not permit this more involved analysis. It is reasonable to assume the effect of the resistance to be significant as it is with the self-saturating circuits[4].

2. The inherent approximation in our assumption of the simplified B-H curve.

3. The use of the constrained half-wave self saturating circuit to derive the control magnetization curve.

In view of the above, we may only consider the analysis certainly as a useful first approximation, and shall go ahead and use it on the Split-Feedback and the Voltage-Doubler, push-pull circuits.

V. Analysis of the Split-Feedback Circuit with 100% Feedback on Basis of Simplified Hysteresis Loop

A, Analysis

The analysis based on the ideal B-H relation resulted in the waveforms of Fig. MRI-13399c. These will not change in the present analysis, which will primarily provide us with the waveform of $i_c = i_{c1} - i_{c2}$, which was zero in the idealized case. The actual B-H excursions are as in Fig. MRI-13408a and approximated in Fig. MRI-13408b.

The mmf equations are repeated here for convenience:

$$h_{1a} = -i_1 N - |i_1|N/2 + |i_2|N/2 - i_{c1}N_c$$

$$h_{1b} = -i_1 N + |i_1|N/2 - |i_2|N/2 + i_{c1}N_c$$

since $N_f = N/2$

$$h_{2a} = -i_2 N + |i_1|N/2 - |i_2|N/2 - i_{c2}N_c$$

$$h_{2b} = -i_2 N - |i_1|N/2 + |i_2|N/2 + i_{c2}N_c$$

In Region M (Fig. MRI-13399c),

$$\Phi_{1b} = \Phi_{o1} \quad \text{and} \quad h_{1b} = -|h_{o1}|.$$

Also,

$$h_{2a} + h_{2b} < 0 \quad \text{and} = -2i_2 N,$$

so that i_2 is positive, as we already know, and

$$h_{2a} = -3Ni_2/2 + i_1 N/2 - i_{c2}N_c; \quad h_{2b} = 1/2\, Ni_2 - 1/2\, Ni_1 + i_{c2}N_c = -|h_{2b}|.$$

$$h_{1b} = -1/2Ni_2 - 1/2Ni_1 + i_{c1}N_c = -|h_{o1}|; \quad i_c = i_{c1} - i_{c2} = 1/N_c(|h_{2b}| - |h_{o1}|).$$

In Region N:

$$\Phi_{2b} = \Phi_{o2}; \quad \Phi_{1b} = \Phi_{o1}; \quad h_{2b} = -|h_{o2}|; \quad h_{1b} = -|h_{o1}|,$$

and since i_1 and i_2 are both positive:

$$h_{2b} = -|h_{o2}| = -i_2 N/2 - i_1 N/2 + i_{c2}N_c; \quad h_{1b} = -|h_{o1}| = -i_2 N/2 - i_1 N/2 + i_{c1}N_c;$$

$$N_c i_c = N_c(i_{c1} - i_{c2}) = |h_{o2}| - |h_{o1}|.$$

In Region O: Almost instantly $h_{1a} + h_{1b}$, $h_{2a} + h_{2b}$, change sign from minus to plus and because $h_{2a} + h_{2b} = -2i_2N$, $h_{1a} + h_{1b} = -2i_1N$, both i_1 and i_2 must be negative, and:

$h_{1a} - h_{2a} = N_c(i_{c2} - i_{c1}) = 0$; $h_{1a} = -i_1N/2 - i_2N/2 - i_{c1}N_c$; $h_{2a} = -i_1N/2 - i_{c2}N_c$.

In Region P: $h_{2a} + h_{2b} > 0$, so that i_2 is negative; $h_{1a} + h_{1b}$ 0, so that i_1 is negative;

$$h_{1a} = |h_{o1}| = -i_1 N/2 - i_2N/2 - i_{c1}N_c;$$

$$h_{2a} = -i_1N/2 - i_2N/2 - i_{c2}N_c; \quad h_{2a} - h_{1a} = h_{2a} - |h_{o1}| = (i_{c1} - i_{c2})N_c.$$

In Region Q: $h_{2a} = h_{o2}$; $h_{1a} = h_{o1}$; i_1 and i_2 are negative; $h_{2a} - h_{1a} = |h_{o2}| - |h_{o1}| = N_c(i_{c1} - i_{c2})$.

In Region R: (analagous to Region O), $h_{1a} + h_{1b} < 0$, so that i_1 and i_2 are each positive;

$$h_{2b} = -i_1N/2 - i_2N/2 + i_{c2}N_c;$$

$$h_{1b} = -i_1N/2 - i_2N/2 + i_{c1}N_c; \quad h_{1b} - h_{2b} = N_c(i_{c1} - i_{c2}) = 0.$$

Regions N and Q end almost at $wt = \pi$ and 2π respectively.

To find N_cI_c:

From A_1 to A_2: $N_cI_c = |h_{2b}| - |h_{o1}|$ ..... Region M.

Also

$$\int_{\Phi_{o1}}^{\Phi_{2b}} d\Phi_{2b} = -(d/2N)V_m \int_{A_1/\omega}^{t} \sin wt\, dt,$$

Therefore

$$\Phi_{2b} - \Phi_{o1} = \Phi_m d/2\,(\cos wt - \cos A_1) \quad A_1 \leq wt \leq A_2$$

$|h_{2b}| - |h_{o1}|$ can now be gotten if the control magnetization curve is available since Φ_{o1} and A_1 are known as function of I.

Thus

$$\Phi_{o1} = \Phi_s - (\Phi_m/2)\left[2 - \frac{I_x(2-d) + Id}{I_m}\right] = \Phi_s - (\Phi_m/2)(1-\cos A_1)$$ See pp.12-13.

Letting

$$k = \left|\Delta \frac{\Phi}{\Phi_s} / \Delta h\right|, \text{ as before,.....}$$

$$|h_{2b}| - |h_{o1}| = (1/k)\frac{\Phi_{o1} - \Phi_{2b}}{\Phi_s} = \frac{\Phi_m d}{2k\Phi_s}(\cos A_1 - \cos wt) = N_c I_c =$$

$$\frac{h_m}{2} d (\cos A_1 - \cos wt), \text{ where } h_m = (1/k)(\Phi_m/\Phi_s).$$

From A_2 to π (Region N);

$$N_c i_c = |h_{02}| - |h_{o1}|$$

$$\Phi_{o2} = \Phi_s - \frac{\Phi_m}{2}\left[2 - \frac{I_x(2-d) - dI}{I_m}\right]; \quad N_c i_c = \frac{1}{k}\frac{\Phi_{o1} - \Phi_{o2}}{\Phi_s}$$

From A_1 to O: $N_c i_c = 0$.... Region R.

Collecting terms and rearranging and averaging:

$$N_c I_c = (1/\pi k)\left[\frac{(\Phi_{o1} - \Phi_{o2})}{\Phi_s}(\pi - A_2) + \frac{\Phi_m d}{2\Phi_s}\left((A_2 - A_1)\cos A_1 + \sin A_1 - \sin A_2\right)\right].$$

Since

$$I = (2V_m/TR_t)\int_{A_1}^{A_2} \sin wt \, dtw/w \ldots\ldots = 1/2\, I_m(\cos A_1 - \cos A_2),$$

$$\Phi_{o1} - \Phi_{o2} = 1/2\, \Phi_m d(\cos A_1 - \cos A_2) = \Phi_m dI/I_m,$$

$$N_c I_c = (\Phi_m d/k\Phi_s \pi)\left[\frac{I}{I_m}(\pi - A_2) + 1/2\left\{(A_2 - A_1)\cos A_1 + \sin A_1 - \sin A_2\right\}\right].$$

To find A_1 and A_2, the following expressions are available...(Pg. 11 Eq. 11)

$$I_x = I + (1 + \cos A_2)\ [I_m/(2-d)],$$

so that

$$\cos A_2 = (I_x - I)\ (\frac{2-d}{I_m}) - 1$$

and

$$\cos A_1 = 2I/I_m + \cos A_2.$$

The procedure in calculating the transfer curve would be to evaluate the circuit parameters d, Φ_m, Φ_s, I_m and k. Values of I would be assumed, A_1 and A_2 found from the above equations and I_c obtained from the last equation on Page 24.

Average Gain ..... for $I_x = I_m$ and $\Phi_m d = 2\Phi_s$.

At

$$I = I_m = I_x,\ N_c I_c = \Phi_m d/2k\Phi_s = 1/k.$$

$$\text{Average Ampere-Turn Gain} = NI/N_c I_c = kNI_m = \frac{1\Delta\Phi N\ I_m}{\Phi_s\ \Delta\ h} = \frac{4wL}{\pi dR_t} = \frac{4Q}{\pi d}.$$

B. Experimental Results

Fig. MRI-13409 contains experimental curves of I versus $N_c I_c$ for various combinations of parameters. The results, using the same values for 'k' as were used in the last chapter, are:

	Experimental	Theoretical
Curve 1, $I_m > I_x$	0.4 Amp-Turns	0.70, 0.50, 0.75
Curve 2, $I_m < I_x$	0.6	1.6, 1.1, 1.7
Curve 3, $I_m \approx I_x$	0.6	1.5, 1.1, 1.7

Similar comments as were made in the last section, apply here.

C. Transient Response and Figure of Merit

The time constant may be derived in the customary manner, which, for the simple circuits, is fairly accurate for low values of control or bias circuit resistance.5 Referring to Fig. MRI- 13397:

$$E_b + E_c = R_b i_{c1} + R_c(i_{c1} - i_{c2}) - N_c(\dot{\Phi}_{1a} - \dot{\Phi}_{1b})$$

$$E_b - E_c = R_b i_{c2} - R_c(i_{c1} - i_{c2}) - N_c(\dot{\Phi}_{2a} - \dot{\Phi}_{2b})$$

$$2E_c = (R_b + 2R_c)(i_{c1} - i_{c2}) - N_c(\dot{\Phi}_{2b} - \dot{\Phi}_{1b} + \dot{\Phi}_{1a} - \dot{\Phi}_{2a})$$

or

$$E_c = R'_c + \frac{N_c}{2}\frac{d}{dI_c}(\Phi_{1b} - \Phi_{1a} + \Phi_{2a} - \Phi_{2b})\frac{di_c}{dt}, \text{ where } R'_c = (1/2R_b) + R_c.$$

If the time constant is large compared with the period of the carrier voltage, average values may be substituted for instantaneous values, so that

$$E_c = R'_c + 1/2\ N_c\ d/dI_c\ (\Phi_{1b} - \Phi_{1a} + \Phi_{2a} - \Phi_{2b})\ dI_c/dt.$$

A somewhat similar order or approximation is involved in substituting for

$$\Phi_{1a} - \Phi_{1b} \quad \text{and} \quad \Phi_{2a} - \Phi_{2b},$$

the expressions

$$-\Phi_s - \Phi_{o1} \quad \text{and} \quad -\Phi_s - \Phi_{o2},$$

which are correct only for

$$R'_c = 0.$$

Now

$$E_c = R'_c I_c + 1/2\ N_c \frac{d}{dI_c}(\Phi_{o1} - \Phi_{o2})\frac{dI_c}{dt},$$

and defining

$$1/2\ N_c\ d/dI_c\ (\Phi_{o1} - \Phi_{o2})$$

as the apparent inductance, we have:

Time Constant = $\tau = L_a/R'_c$ with $L_a = (1/2)N_c \frac{d}{dI_c}\frac{\Phi_m I_d}{I_m} = (1/2)N_c\ \Phi_m/I_m(d)\ dI/dI_c$.

We will use the average value of I/I_c, but must note that it depends on the relative values of I_x and I_m. For the case $I_x = I_m$, representing the best practical situation, the average gain = $4Q/d\pi = NI/N_c I_c$, so that $L_a = 1/2\ N_c(\Phi_m/I_m)(dN_c/N\pi)(4Q/d) = (N_c^2/N^2)L = L_c$, i.e., the inductance as seen from the control side, so that $\tau = L_c/R'_c$, and the

Figure of Merit = Power Gain/Time Constant = $F^2I^2R/R'_cI_c^2 = \tau$

$16F^2RwQ/d^2R_t\pi^2$ (where $Q = wL/R_t$) $= 1.6F^2RwQ/(d^2R_t) = (d-1/d^2)\ 1.6F^2wQ$, for this case where $I_x = I_m$ and $\Phi_m d = 2\Phi_s$, and where F = Form factor.

D. Experimental Work

Fig. MRI-13411b consists of copies of transient responses photographed with the aid of a 60-cycle integrator[6] which operates by integrating over one cycle, indicating the result during the next cycle, while a twin circuit integrates over this latter cycle and indicates its result while the other is integrating. In this way a good approximation to the true average output current may be obtained. The dotted lines are true experimental curves, thus indicating the divergence of the latter from true exponentials.

The theoretical and experimental time constants are herewith listed:

		Experimental	Theoretical
1A	Rise	0.13 seconds	0.09 seconds
1B	Fall	0.15	
2A	Rise	0.15	0.13
2B	Fall	0.25	
3A	Rise	0.31	0.31
3B	Fall	0.50	
4	Rise	0.22	0.25
5A	Load consists of R + jX = 118 + j250 (air-cored) - Rise		
6	Rise - Load consists of 85 + j250 ohms.		

In all of the above experimental average gain was used to predict the time constant.

In the next section, a similar analysis is made of the Push-Pull Voltage Doubler circuit, in order to compare it with the Split-Feedback circuit.

VI. Analysis of the Push-Pull Voltage Doubler

A. Analysis

This analysis will be based upon the same simplified B-H hysteresis loop that was used in the last section. The circuit diagram is drawn in Fig. MRI-13411a. The mmf equations are:

$h_{1a} = Ni_{1a} - N_c i_{c1}$; $h_{1b} = Ni_{1b} - N_c i_{c1}$;

$h_{2a} = Ni_{2a} - N_c i_{c2}$; $h_{2b} = Ni_{2b} - N_{ci} i_{c2}$;

For $R_b = R_c = 0$, $\Phi_{1a} + \Phi_{1b} = K_1 = \Phi_s + \Phi_{o1}$, where $|\Phi_{o1}| < \Phi_s$

$\Phi_{2a} + \Phi_{2b} = K_2 = \Phi_s + \Phi_{o2}$, where $|\Phi_{o2}| < \Phi_s$, with

the customary limitations on the circuit parameters.

We may begin by assuming Core 1_a is saturated and 2_a is unsaturated, this condition existing for $A_1 \leqslant wt \leqslant A_2$.

$$i_{1a} = v/R_t,$$

so that $i_{1b} = 0$, if the rectifiers are perfect[7].

$$h_{1b} = -|h_{o1}| = N_c i_{c1}(-1);$$

$\dot{\Phi}_{2a} = vd/N$, with 'v' positive. In Fig. MRI-13411b, this part of the cycle is shown as Region M.

At $wt = A_2$, Φ_{2a} saturates and $i_{1a} = i_{2a} = v/r$; $\Phi_{2b} = \Phi_{o2}$; $-|h_{o2}| = -N_c i_{c2}$ since $i_{2b} = 0$, while $|h_{o1}| = N_c i_{c1}$. This is Region N for $A_2 \leqslant wt \leqslant \pi$, in Fig. MRI-13411b. This ends when either

$$h_{1a} = Nv/r - |h_{o1}| = -|h_x| \text{ or } h_{2a} = nv/r - |h_{o2}| = -|h_x|,$$

which occurs very nearly at $wt = \pi$.

For

$$(\pi + A_1) \geqslant wt \geqslant \pi, \quad v = N\dot{\Phi}_{1a} = -N\dot{\Phi}_{1b} = -N\dot{\Phi}_{2b}.$$

Integrating,

$$\Phi_{1a} - \Phi_s = -\Phi_m(1 + \cos wt) = \Phi_{2a} - \Phi_s.$$

$$\Phi_{2b} = \Phi_s + \Phi_{o2} - \Phi_{2a} = \Phi_{o2} + \Phi_m(1 + \cos wt).$$

Because of the nature of approximation of the B-H loop, almost at onec $h_{2b} - h_{2a} > 0$, so that $i_{2b} - i_{2a} > 0$ and $i_{2a} = 0$, as only one branch can conduct. Therefore $h_{2a} = -N_c i_{c2}$ and similarly $i_{1a} = 0$, $h_{1a} = N_c i_{c1}$. The preceding constitutes Region 0, i.e., $\pi + A_1 \geqslant wt \geqslant \pi$.

For $\pi + A_2 \geqslant wt \geqslant \pi + A_1$, region P,

$\Phi_{1b} = \Phi_s$, $\Phi_{1a} = \Phi_{o1}$, $i_1 = v/R_t$, $|h_{o1}| = N_c i_{c1}$, $\dot{\Phi}_{2a} = vd/N$.

Integrating....

$$\Phi_{2a} = \Phi_{o1} - \Phi_m d\,(\cos wt + \cos A_1), \text{ with } h_{2a} = -N_c i_{c2}.$$

For $2\pi \geqslant wt \geqslant \pi + A_2$, (Region Q):

$\Phi_{2b} = \Phi_s = \Phi_{1b}$; $i_1 = i_2 = v/r$; $\Phi_{1a} = \Phi_{o1}$; $\Phi_{2a} = \Phi_{o2}$;

$h_{1a} = -|h_{o1}| = -N_c i_{c1}$; $h_{2a} = -|h_{o2}| = -N_c i_{c2}$.

<u>Summarizing:</u>

From π to $\pi + A_1$: $i_{c1} - i_{c2} = 0 = i_1 - i_2$. $\Phi_{1a} = \Phi_{2a} = \Phi_s = \Phi_m(1 + \cos wt)$

$h_{1a} = -N_c i_{c1} = h_{2a} = -N_c i_{c2}$ and $i_{c1} = i_{c2} = (1/N_c)\left[|h_x| + |h_m|\,(1 + \cos wt)\right]$.

From $\pi + A_1$ to $\pi + A_2$: $i_1 = v/R_t$, $i_2 = 0$, $\Phi_{2a} = \Phi_{o1} - \Phi_m d\,(\cos wt + \cos A_1)$,

$i_{c1} = |h_{o1}|/N_c$; $N_c i_{c2} = |h_{o1}| + |h_m| d\,(\cos wt + \cos A_1)$.

From $\pi + A_2$ to 2π: $i_1 = i_2 = v/r$; $i_{c1} = |h_{o1}|/N_c$; $i_{c2} = |h_{o2}|/N_c$.

We also have the following relations:

$|h_{o1}| = |h_x| + |h_m|\,(1 - \cos A_1)$; $I = 1/2\, I_m\,(\cos A_1 - \cos A_2)$.

$\Phi_{o2} - \Phi_{o1} = -\Phi_m d\,(\cos A_1 - \cos A_2) = -\Phi_m d\, 2I/I_m$.

$|h_{o2}| - |h_{o1}| = 2d\,|h_m|\, I/I_m$.

$$wN_c(1/2T(I_{c2} - I_{c1}) = \int_{\pi+A_1}^{\pi+A_2} d|h_m|(\cos wt + \cos A_1)d(wt) + \int_{\pi+A_2}^{2\pi} (h_{o2} - h_{o1})d(wt).$$

$$I_c = h_m/N_c \left[(\pi - A_2)|h_{o2} - h_{o1}|/h_m + d(\sin A_1 - \sin A_2) + d \cos A_1(A_2 - A_1)\right]$$

$$I_c = (1/kN_c\Phi_s\pi)(2\Phi_m d) \left[(\pi - A_2)I/I_m + \frac{(A_2 - A_1)\cos A_1 + (\sin A_1 - \sin A_2)}{2}\right]$$

which is exactly twice the expression for the Split Feedback circuit, on Page 24. If the same cores are used for the two circuit, then $N_{v.d.} = 2N_{s.f.}$, However, for the Doubler circuit (for the case $I_{max} = I_m$, $\Phi_{md} \leq \Phi_s/d$, while for the Split Feedback circuit, $\Phi_{ms.f.} \leq 2\Phi_s/d$.

Since $\Phi_{ms.f.} = V_m/wN$, and $\Phi_{m\,d} = V_m/2wN$, V_m and consequently I_m are the same for both circuits. And as $\Phi_{md} = 1/2\Phi_{msf}$, the expressions for I_c are actually the same for both circuits.

The equations for I_{c1} and I_{c2} may also be gotten:

$$T/2\ wN_cI_{c1} = \int_{\pi}^{\pi+A_1} h_x + h_m(1 + \cos wt)\ dtw + \int_{\pi+A_1}^{2\pi} h_{o1}\ dtw, \text{ therefore}$$

$$\pi N_cI_{c1} = A_1(|h_x| + |h_m|) - |h_m| \sin A_1 + |h_{o1}|(\pi - A_1), \text{ and}$$

$$I_{c2} - I_{c1} = I_c.$$

B. Excess Currents

The transcendal equations above permit no simple solution. We may note however that at $I_c = 0$,

$$N_cI_{c1} = \pi N_cI_b = A_o(|h_x| + |h_m|) - h_m \sin A_o + |h_{o1}|(\pi - A_o),$$

which is exactly the expression for the single mesh doubler circuit, for the same B-H assumption. Thus $A = A_o$; the conduction angle, at zero input, is the same for the push-pull connection as it would be if the same amount of bias ampere-turns were applied to a single mesh. And because the circulating current is a maximum at zero control current we can now determine the excess current = $1/2\ I_m'(1 + \cos A_o) - I_m$. At zero control current, with the single mesh, $I_o = 1/2\ I_m(1 + \cos A_o)$, so that excess current = $(I_m' I_o/I_m) - I_m$, where I_o is simply the output current in a single mesh for that value of Control (or Bias) Ampere-turns equal to the Bias Ampere-turns used in the Push-Pull circuit.

The average gain of the Push-Pull circuit may be found by finding I_c at $A_1 = 0$ and at $A_2 = \pi$. The result is $N_c I_c = \Phi_m d/k\Phi_s$, and setting $\Phi_m = \Phi_s/d$, the best practical value, $N_c I_c = 1/k$, exactly the same as for the Split Feed back circuit for the case $I_x = I_m$, and $\Phi_m = 2\Phi_s/d$.

This gain (for the Doubler circuit) is achieved only at the expense of very large excess currents for it is found that the bias ampere turns for this case = $h_x + 1/2\ h_s$, which results in a conduction angle (for a single mesh) in the neighborhood of 90°. Actually, a transcendental equation must be solved for this angle, namely,

$$\pi N_c I_c = \pi(h_x + 1/2\ h_s) = A_o(|h_x| + |h_s|/d) - |h_s| \sin A_o/d$$

$$+ \left[(|h_x| + |h_s| (1 - \cos A_o)\right] (\pi - A_o)/d$$

$$= A_o(h_x + h_s/d) - h_s \sin A_o/d + \left[h_x + h_s (1 - \cos A_o)/d\right] (\pi - A_o).$$

finally yielding, $\pi d/2 = \pi - \sin A - (\pi - A) \cos A$.

In short, on account of the excess currents involved, this value of gain is not realizable. We will compare the relative merits of the two push-pull circuits in more detail in the last section. It is interesting, however, to note that aside from the excess currents, there is a remarkable similarity between the two, which extends to the transient response as will now be shown.

C. Transient Response

Referring to Fig. MRI-13411a,

$$E_b - E_c = (R_b + R_c)\ i_{c1} - R_c i_{c2} - N_c(\dot{\Phi}_{1a} + \dot{\Phi}_{1b})$$

$$E_b - E_c = -R_c i_{c1} + (R_b + R_c)\ i_{c2} - N_c\ (\dot{\Phi}_{2a} + \dot{\Phi}_{2b}).$$

$$E_c = R'_c\ i_c + 1/2\ N_c\ d/di_c\ (\Phi_{1a} + \Phi_{1b} - \Phi_{2a} - \Phi_{2b}) di_c/dt.$$

Substituting and approximating exactly as with the split-feedback circuit:

$$E_c = R'_c\ I_c + (N_c \Phi_m d/I_m)\ (dI/dI_c)\ (dI_c/dt).$$

We need proceed no further than to note that the parameters hare are the same as for the other circuit. (There - $1/2dN_c\Phi_m/I_m dI/dI_c$, but Φ_m there is twice Φ_m here.)

D. Experimental Work

Fig. MRI-13409 presents a curve (marked V.D.) of output current for circuit parameters corresponding to those of the Split Feedback circuits. It is seen that the gain is less as expected when the bias is not adjusted for maximum gain on account of the very large excess currents which would then flow. Further experimental results of this nature are posponed to the last section where they are compared with the results for the Split-Feedback circuit.

Fig. MRI-13411b presents transient response curves of the Push-Pull Doubler for various parameter values. The theoretical and experimental values of the time constant are:

	Theoretical	Experimental
No. 7A - Rise	0.12 seconds	0.16 seconds
7B - Fall		0.12
8A - Rise	0.054	0.042
8B - Fall		0.033

VII. The Split-Feedback Amplifier Compared to the Voltage Doubler Amplifier

A. Design Figure of Merit

To compare the two circuits, a Design Merit Figure may be defined equal to the Power Gain of a circuit divided by the Copper Core losses. For the two amplifiers, we assume identical cores and loads in order that this factor have meaning.

It will be necessary to decide what windings, such as the control and bias, may be neglected in calculating the core copper losses. For the V.D., the bias and control windings are neglected here, while the latter winding only is neglected for the S.F. circuit.

For the S.F. circuit it is very reasonable to assume optimum operating conditions as they are easily achieved - that is, $I_x = I_m$. One must make some assumption as to the operating conditions of the V.D. circuit, since adjustment of bias for maximum gain will result in large excess current. For this present comparison, we assume the

bias is such that at zero control input, $I_{circulating} = I_m$, so that the Power Gain is only 1/4 the maximum Power Gain.

We also take the maximum gain of the two circuits to be equal. Our theoretical analysis have indicated this to be correct. Experimentally we have found that for circuit conditions very similar, the S.F. circuit gain is higher than the V.D. circuit gain. These results are presented in Figures MRI-13412a, MRI-13412b, MRI-13413a and MRI-13413b inclusive. It is assumed that the lower gain of the V.D. circuit is due to the fact that the bais has been adjusted to reduce the large circulating currents and with these, - gain.

It may be shown[8] that for a constant winding area, the copper dissipation in the core, is to a good approximation, proportional to $I_{rms}{}^2 N^2$. At what point in the cycle is the dissipation, i.e., I_{rms}, a maximum ? For both amplifiers this occurs at the quiescent point, when $I_c = 0$, when the circulating currents have their highest values. The flow angle is small, the peak current large so that RMS value (for the same average) is higher. This is analytically convenient, anyway, for it makes our calculations independent of control current input.

The conduction angle at zero control input is a function only of 'd', i.e., <u>for the S.F. circuit:</u>

$$(2/T) \int_{A_o}^{\pi} (V_m/r) \sin wt \frac{dt\omega}{\omega} = 1/2 I_m, \text{ so that } \cos A_o = (r/R_t) - 1.$$

$$I_{rms} = \sqrt{(2/T) \int_{A_o}^{\pi} (V_m^2/r^2) \sin^2 wt \frac{dt\omega}{\omega}} = \frac{I_m'}{\sqrt{8}} \sqrt{(\pi - A_o + 1/2 \sin 2A_o)\, \pi}$$

and the dissipation is $K(N_b^2 I_{brms}^2 + 4N^2 I_{rms}^2) = 5KI_{rms}^2 N^2$, since

$$I_{brms} = I_{rms}\, N/N_b \text{ at } I_c = 0.$$

<u>For the Doubler Circuit:</u>

$$(2/T) \int_{A_o'}^{\pi} (V_m/r) \sin wt \frac{dt\omega}{\omega} = I_m, \text{ resulting in } \cos A_o' = 2r/R_t - 1,$$

and

$$I_{rms}' = \frac{I_m'}{4} \sqrt{\pi\, (\pi - A_o' + 1/2 \sin 2A_o')},$$

because the current flows in each winding for half a cycle only. The dissipation = $4KI'^{2}_{rms}N^2$. At $r = R_t$, the dissipation is almost the same for both circuits, while for r/R_t small (customary situation), the ration of the dissipations

$$\text{S.F. to V.D.} = \frac{2.5\sqrt{2}}{4} \frac{(1 - r/4R_t)}{(1 - r/2R_t)},$$

which for $r/R_t = .10$, means 10% less dissipation for the S.F. amplifier. The limit as $r/R_t \longrightarrow 0$, is approximately 12% less dissipation for the S.F. circuit. Therefore the Design Merit Figure of The Split Feedback Amplifier is more than 4 times as great as that of the Voltage Doubler Push-Pull Amplifier.

B. Sensitivity to Bias Current Variations

The V.D. Amplifier circulating current at $I_c = 0$, is very sensitive to Bias current. A decrease of x% in the bias current will cause an approximate increase in the circulating current of the Gain times x%. This is a serious matter and necessitates conservative design, since for example if the Current gain is 100, a 5% decrease in Bias results in 5 times as much circulating current, and since the normal circulating current at this point has a minimum value of approximately I_m - the result is $5I_m$ for a 5% change in bias current. The amplifying range will be affected by x%.

In constrast, for the Split-Feedback circuit, if the bias is gotten from the line voltage which supplies the load circuit, then any change in line voltage affects I_x and I_m to the same degree, so that the range is unaffected while the circulating current at $I_c = 0$, will be affected only to the extent of x%. Thus a 5% increase in Bias current will increase the Circulating current by 5% only. If the two supplies are independent, the range is affected by x%/Gain.

C. Ease of Bias Adjustment

It is clear that the Voltage Doubler circuit requires very careful bias current adjustment. If it is too large, while it will reduce $I_{circulating}$, it will result in serious non-linearities in the transfer curves. In addition the possible line voltage variations must be considered. If the bias is too small, the circulating currents will be very large. In considering these factors and the possible line voltage variations, the permissible bias range narrows down.

On the other hand the bias adjustment for the Split Feedback circuit is simplicity itself. One can find I_m very easily and then makes $I_x = 2N_bI_b/N = I_m$. And if one is off somewhat, it is not a serious matter.

D. The Saturated Range

Again the Split-Feedback amplifier has superior characteristics. One can, by slightly sacrificing output, obtain a constant output for some portion of the saturated range, or alternatively a slowly rising output (at the rate of r/R_t) over some range, or if maximum output is used, a slowly decreasing output, at the rate of r/R_t, in the saturated range. In contrast, the Voltage Doubler output drops at the rate of unity in the saturated range.

E. Possible Disadvantages

One of these might be the added complexity, which however is only superficial. For the same total number of turns, four more leads must be brought out - i.e., a total of 10 leads compared to 6 for the V.D. For experienced coil winders this is a minor matter indeed.

Another disadvantage might be the fact that a total of 8 rectifier units (4 per bridge) are needed as compared to 4 units for the V.D. However, each of these units in the S.F. circuit has a very low inverse voltage applied to it (zero for R_c or $R_b = 0$) and so may consist of one plate only. The inverse voltage for the V.D. is easily seen to be "ir" and the instantaneous maximum value of this depends upon 'd' since 'i' is greatest at zero control current. If 'd' is small, the r.m.s. value of the current is greater, even though the peak value is smaller - so that it is quite likely that one plate will not suffice.

In addition, in the amplifying range, the maximum value of the RMS current through each rectifier is less (considerably less for r/R_t small) for the Split-Feedback amplifier than for the Voltage Doubler. For example, for $R_t/r = 10$, I_{rms}^2 (of S.F. rectifier) = 0.35 I_{rms}^2 (of V.D. rectifier). Therefore as far as heating ratings are concerned, for this value of R_t/r, the S.F. rectifier need have only 1/3 the ratings of the V.D. rectifier. It is quite likely, thus, that even in this respect, the S.F. circuit compares favorably with the Doubler circuit.

APPENDIX

Data for Fig. MRI-13400a

I_m = 430 m.a. I_x = 300 m.a. $N_c = N = N_b = 400$

$R_t/r = 4.6$; $I_{s2} = I_{s1} + 2(N/N_c)(R_t/r)(I_m - I_x) = I_{s1} + 2 \times 4.6 \times 130 = I_{s1} + 1200$m.a.

Fig. MRI-13400b

$I_m = 250$; $I_x = 300$ m.a. $R_t/r = 4.3$; $I_m' = 1075$m.a. $d = 1.8$

$I = I_m$ at $I_{s5} = I_{s4} + (2/N_c)(N_b I_b - bNI_m) = I_{s4} + 2(150 - 1/2\ 250)$.

Rate of decrease of $I = (N_c/N) \times 1/(b + R_t/r) = 1/(1/2 + 4.3) = 0.2$

Fig. MRI-13400c

Limit of Amplifying range at $I = (2I_m - I_x r/R_t)/(2 - r/R_t)$

$= 286 - 16.4/312/(2-1/3.2) = 138$m.a. - 55.2 A.T.

Increases until $I = I_m$ at $I_c = I_{s4} + (N/N_c)(I_x - 2bI_m) = I_{s4} + 210$ m.a.

$N_c I_c/2 = 40 \times 0.21 = 8.4$ A.T.

Rate of decrease thereafter $= 1/(b + R_t/r) = 1/3.7 = 0.27$

Fig. MRI-13394

$N = N_c = 400$; $N_b = 100$. $r = 9.0 + 2r_{f1}$ (rectifier forward res.)

$R = 109 + 2r_{f2}$. $I_x = 2 \times 100/400 \times 483 = 242$m.a.

$$I_m = \frac{2\sqrt{2}\ (15.8)}{nR_t} = \frac{14.2}{R_t}.$$

Limit of Amp. Range: (70 m.a.). r_{f1} (at 70 m.a.) = 7.4, r = 24, R = 124,

$R_t = 148$, $I_m = 96$ m.a.

$I_c = (I_m N/N_c - I_b 5\ N_b/R_t N_c)(1 - r/2R_t) = 82$m.a.

Rate of slow increase and decrease: r_f (on basis of 100 m.a.) = 5.5 therefore $R_t = 140$, r_f on basis of I_m', = 2.5, r = 14; $r/R_t = 0.10$.

Fig. MRI-13395

I_m I_x, I_x = 2 x 100 x 153/400 = 76 m.a., which is amp. limit.

Limit of saturation and beginning of decrease of I_g at:

$I_c = NI_x/N_c + 2(I_m - I_x)\, R_t\, N/rN_c = 78 + 2\,(103 - 78)\, 140/14 = 571$ m.a.

Fig. MRI-13406

Φ_o/Φ_s as function of N_c I_c from half-wave circuit:

$R_t = R + 4r_f = 98 + 4r_f$. $I_m = 120$ m.a. $V_m = \sqrt{2}$ 16 volts.

$r_f = 5.5\Omega$

I_m is variable on account r_f is a variable. The average currents are used to find r_f.

$\Phi_o/\Phi_s = 1 - 2(\Phi_m/\Phi_s)(1 - 2I/I_m)$. $\Phi_m/\Phi_s = 16/19$

I_c	N_cI_c	I	r_f	I_m	$2I/I_m$	Φ_o/Φ_s
1	0.4	59.8		120	.997	.995
2	0.8	58.3		120	.97	.95
3	1.2	57.7		120	.96	.93
4	1.6	56.0		120	.93	.88
5	2.0	49.0	6.0	118	.83	.7
6	2.4	32.0	8.0	111	.58	.29
7	2.8	12.7	18.0	85	.30	-.18
7.21	2.88	7.6	28.5	57	.267	-.23

$$k = \Delta \frac{\Phi_o}{\Phi_s} / \Delta h = \frac{.80 + .23}{2.89 - 1.825} = 0.97$$

Similarly for the other two curves in this Figure.

Fig. MRI-13407

Experimental 100% series feedback run:

$N = N_f = 400$; $N_c = 100$; $R_t = 163 + 7.3 + 2r_f$. At $I = 150$. $r_f = 4$.

$I_m = \frac{2\sqrt{2} \times 30}{178\pi} = 152$ m.a. $R_t = 178$. $\Phi_s/\Phi_m = 19/30 = 0.633$.

Avarage output/amp-turn input = $[2k\Phi_s/\Phi_m](I_m)$ giving theoretical values.
Experimentally - 100 - 11.6/(2.2 - 0.8) = 70.

Fig. MRI-13409 Curve 1

$I_x = 2(100/400) \times 200 = 100$ m.a.; $\Phi_m/\Phi_s = 25/19 = 1.3$

$R = 100$, $r = 13 + 4r_f = 35$. $d = 1 + 100/135 = 1.74$

$\sin A_1 = 200/266 - 1 = 0.2$; $N_c I_c = d\Phi_m \, 1/2 \, (\pi - A_1) \cos A_1 + \sin A_1 / k\pi\Phi_s = 0.48/k$.

Fig. MRI-13409 Curve 2

$I_x = 200$. $I_x > I_m$. All other parameters as for Curve 1.

$\cos A_2 = 2(I_x - I_m)(2 - d)/I_m d - 1 = -0.94$

$N_c I_c = \Phi_m d \left[I/I_m (\pi - A_2) + 1/2 \, (A_2 - \sin A_2) \right] / k\pi\Phi_s = 1.1/k$

$I_{max} = \left[2 \, (I_m) - I_x (2 - d) \right] / d = 160$ m.a.

Fig. MRI-13410 No. 1a

$R = 86 + 30 = 116$; $r = 13 + 50 = 63$. $R_{eff} = 261 \, N_c^2 \, 9.7/N_b^2 = 49$

where $R_c = 261$, and $R_b = 9.7$.

Theoretical Time Constant: $L = 1/2N_c d\Phi_m/I_m(dI/dI_c) = \dfrac{N_c(R + R_t)dI}{4wN \qquad dI_c}$

$= 0.52 \, 10^{-3} \, 295 \times 57/2 = 4.38$ H.

$= 4.38/49 = 0.09$ seconds, etc.

BIBLIOGRAPHY

(1) Milne, A.G.: Magnetic Amplifiers, Proc. IEE, 96, Part 1, p. 89, (1949).

(2) Gale and Atkinson: A Theoretical and Experimental Study of the
(5) Series-Connected Magnetic Amplifier, Ibid, 96, Part 1, p. 99 (1949).

(3) Smith, E.J.: A Study of Self-Saturated Magnetic Amplifiers, Part 1, MRI Report R-229-49, PIB-174, p. 7, Dec. 30, 1949.

(4) Smith, E.J.: A Study of Self-Saturated Magnetic Amplifiers, Part 3, MRI Report R-231-50, PIB-176, March 27, 1950.

(6) Roman, S.: A Cyclic Integrator, MEE Thesis, Polytechnic Institute of Brooklyn, May, 1951.

(7) Erkman, A.: The Steady State and Transient Analysis of the Doubler and Full-Wave Magnetic Amplifier, MRI-Report R-260-51, PIB-201, p.5, Oct. 25, 1951.

(8) Reyner, J.H.: The Magnetic Amplifier (Book), Stuart and Richards, London, p. 80, 1950.

(9) Kabrisky, M.J.: The Use of Magnetic Amplifiers to Drive Two-Phase Servo Motors, MEE Thesis, Polytechnic Institute of Brooklyn, Chapter 3, and Figs. 15 to 18, June, 1952.

A.

SPLIT-LOAD CIRCUIT

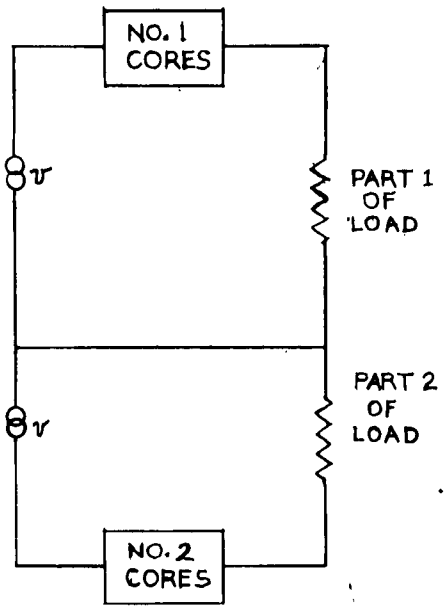

B.

2-TERMINAL LOAD CIRCUIT

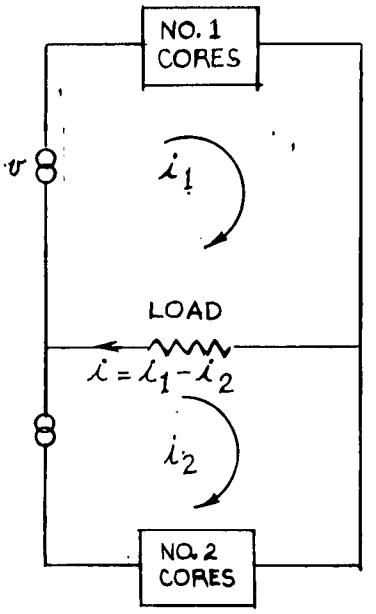

C.

2-TERMINAL LOADS WITH MIXING RESISTORS

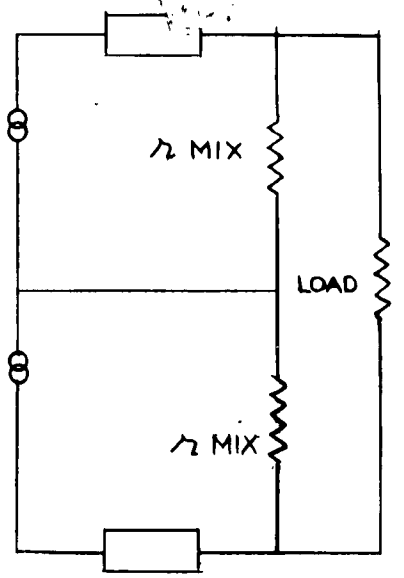

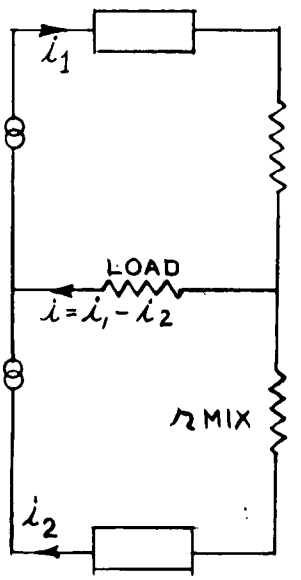

MRI - 13389

UNCONSTRAINED MAGNETIC AMPLIFIER(PP) WAVEFORMS

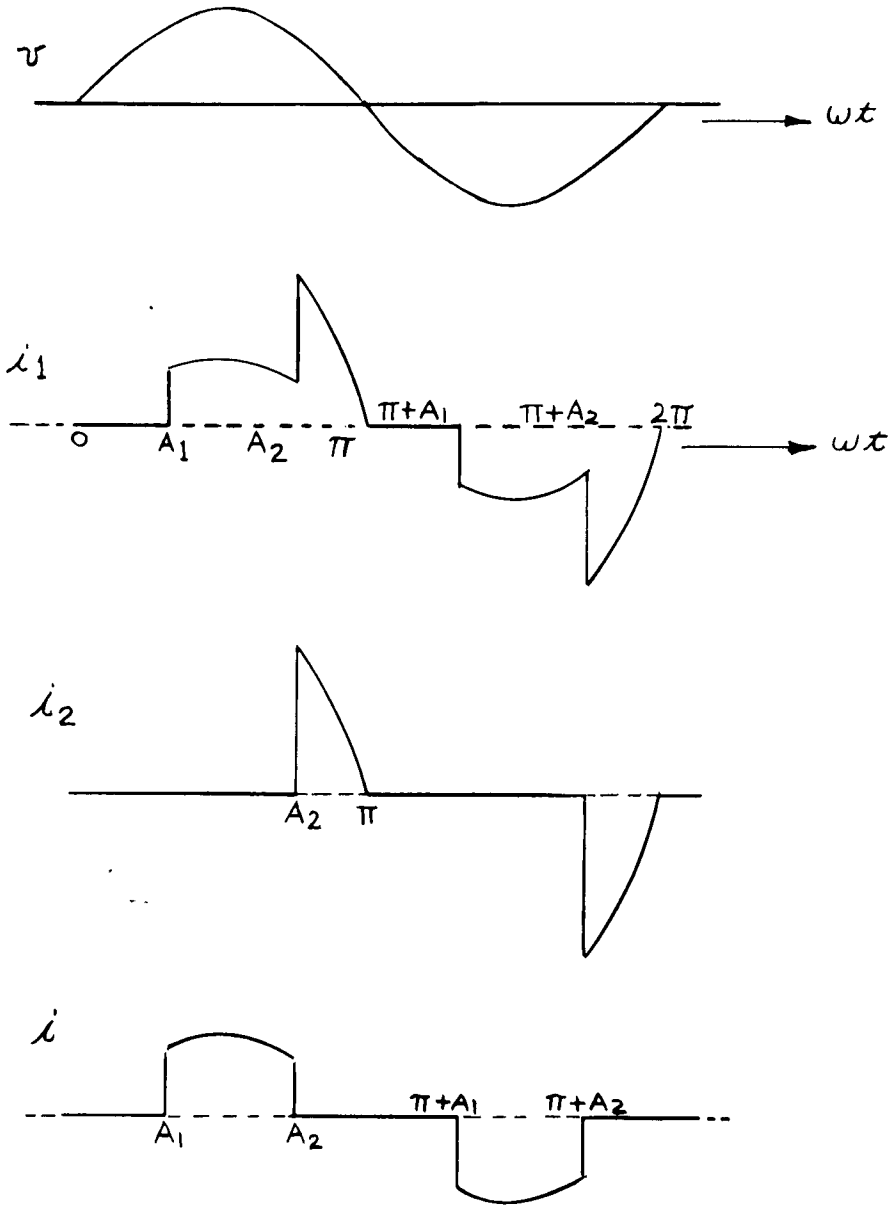

MRI -13390

A.

A.C. PUSH - PULL CURRENT AMPLIFIER

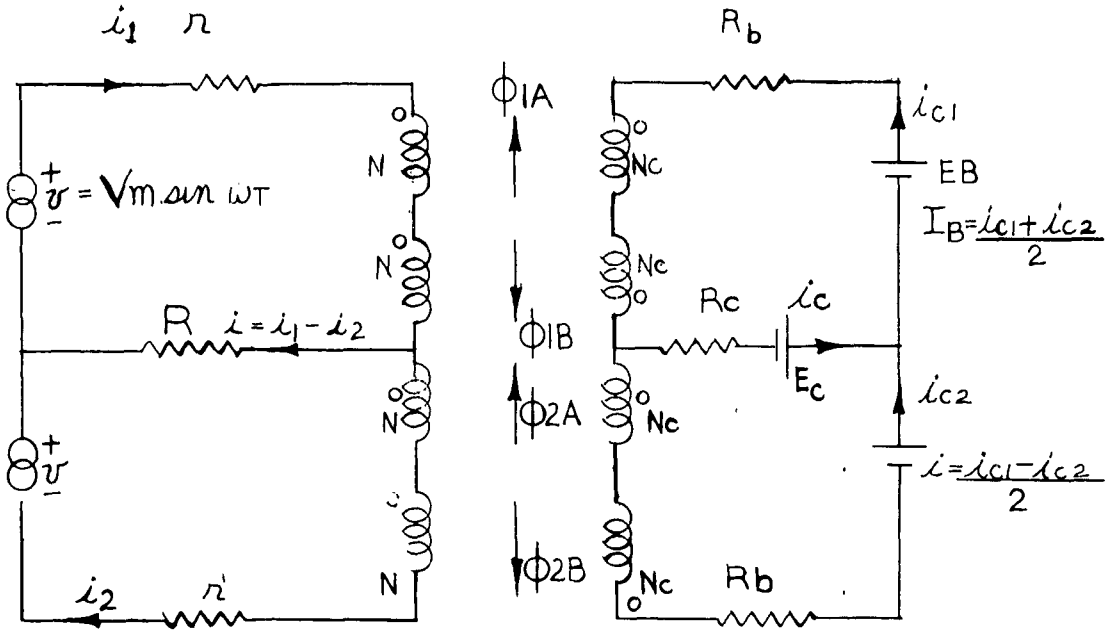

B.

IDEAL B-H CHARACTERISTIC

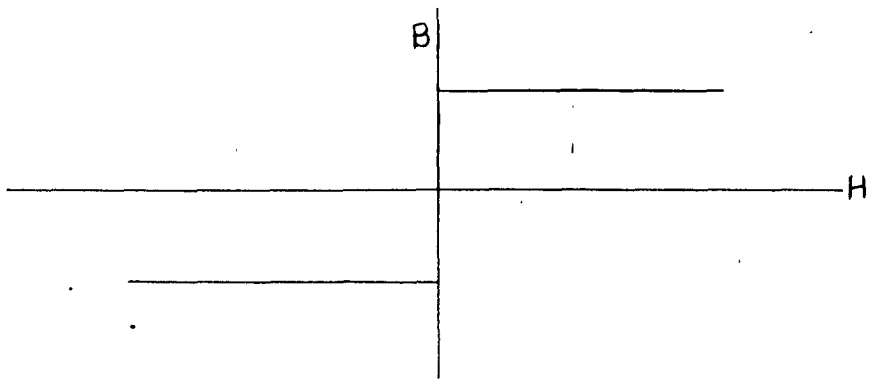

MRI - 13391

A.
COMB'N. 1 WAVEFORMS

B.
COMB'N 2 WAVEFORMS

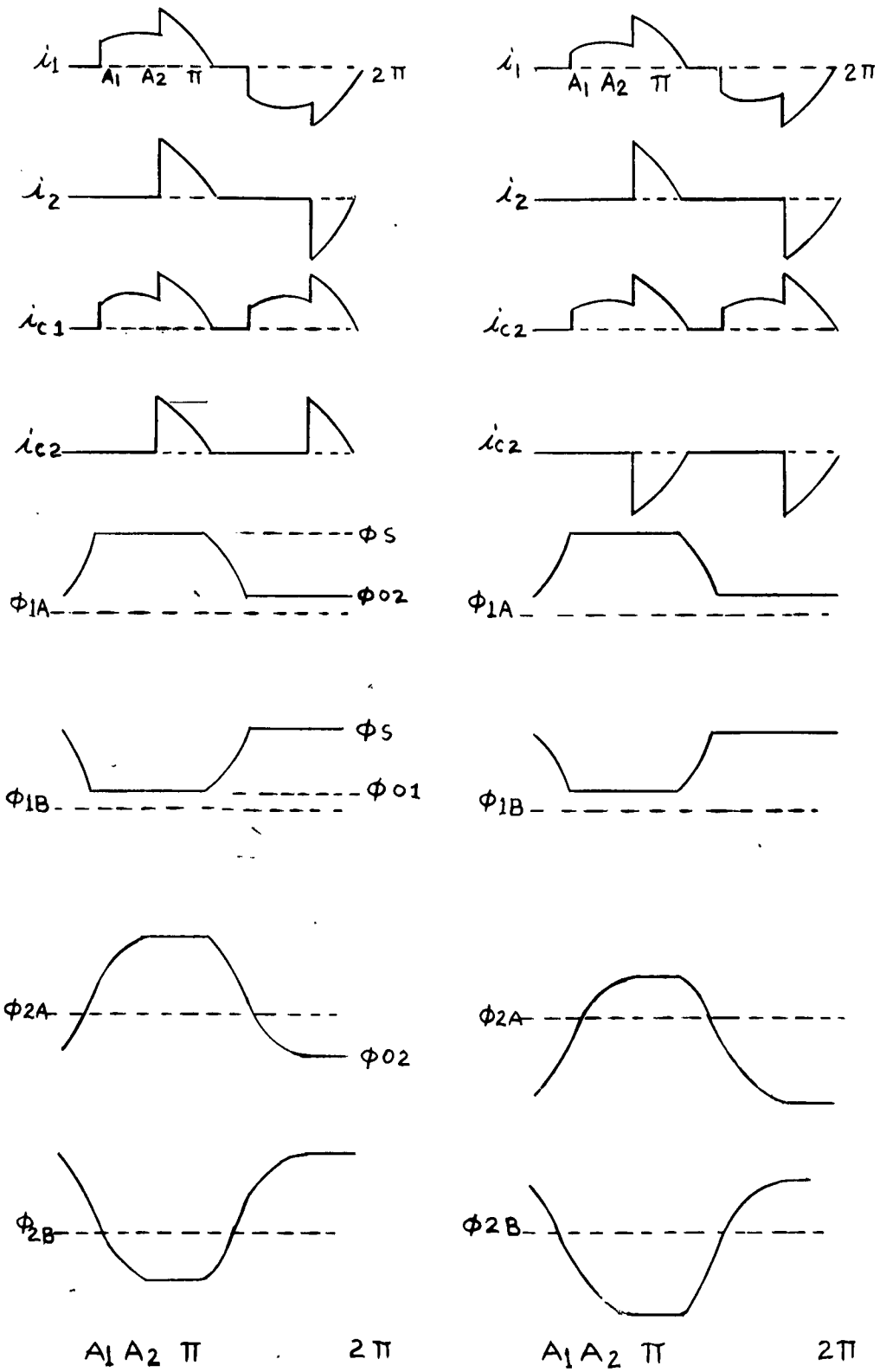

MRI - 13392

A.

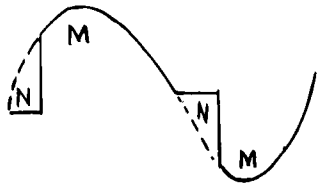

$I_m = M+N$. WHEN $I_m > I_x$, & $A_2 = \pi$, $I_x = M$

B.

C.

SATURATED RANGE WAVEFORMS.

D.

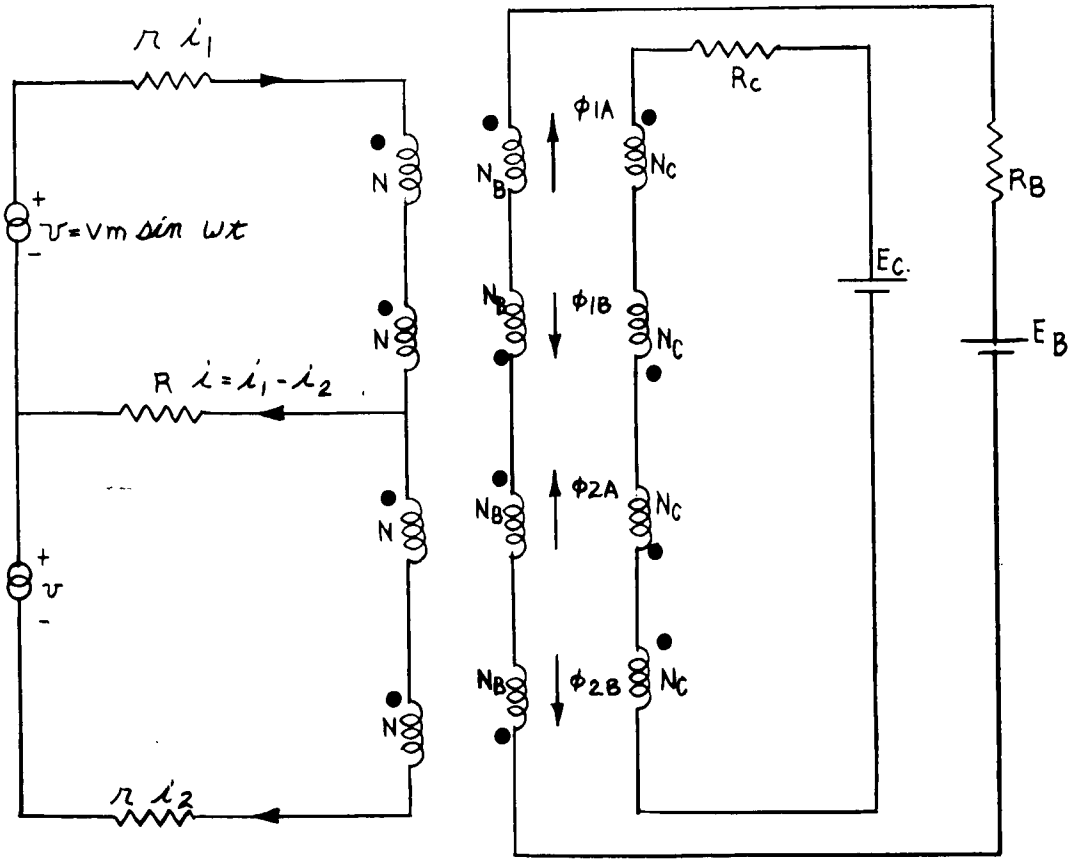

SEPARATE BIAS & CONTROL WINDINGS

MRI - 13393

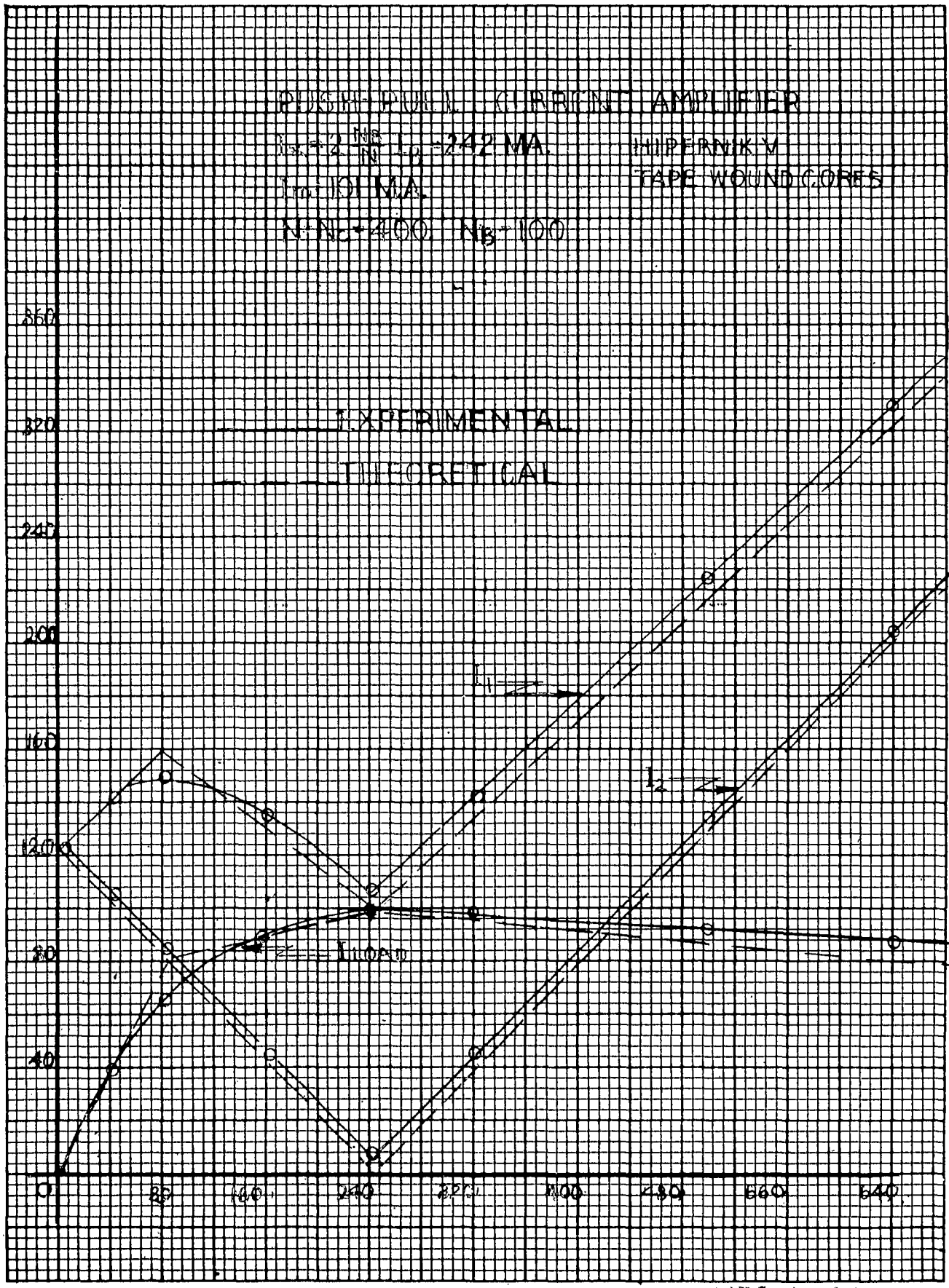
PUSH-PULL CURRENT AMPLIFIER
$I_{b1} = 2\frac{N_B}{N} I_b = 242$ MA.
$I_{b2} = 101$ MA.
$N = N_C = 2400$, $N_B = 100$
HIPERNIK V
TAPE WOUND CORES
EXPERIMENTAL
THEORETICAL
360
320
240
200
160
120
80
40
0
80
160
240
320
400
480
560
640
I_1
I_2
I_{load}

MRT - 13394

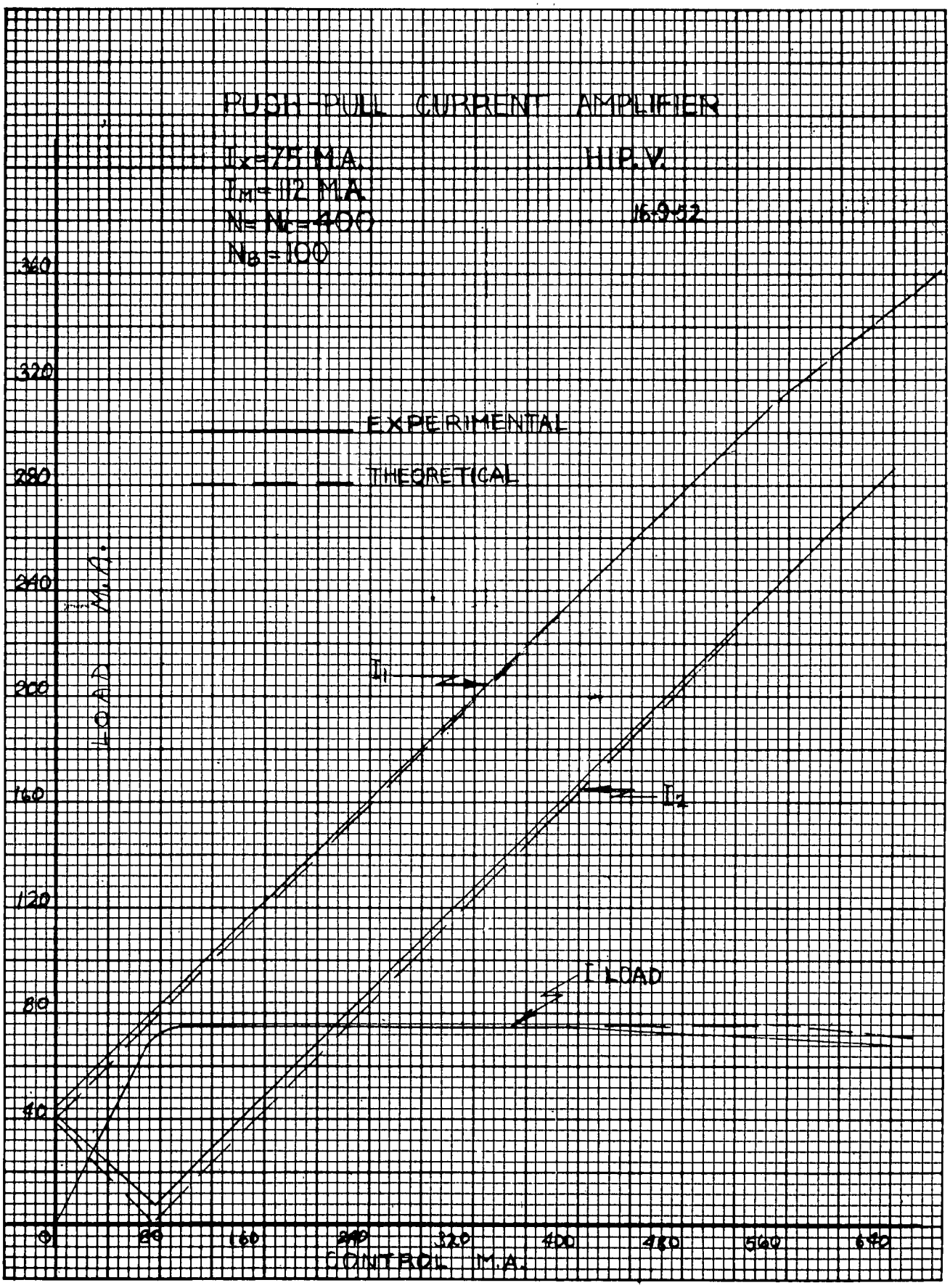
PUSH-PULL CURRENT AMPLIFIER
Ix=75 MA.
IM=112 MA.
N=N'=400
N6=100
H.P.V.
16-952
EXPERIMENTAL
THEORETICAL
I LOAD MA.
I1
I2
I LOAD
360
320
280
240
200
160
120
80
40
0
80
160
240
320
400
480
560
640
CONTROL M.A.

MRI - 13395

P.P. CURRENT AMPLIFIER - WAVEFORMS

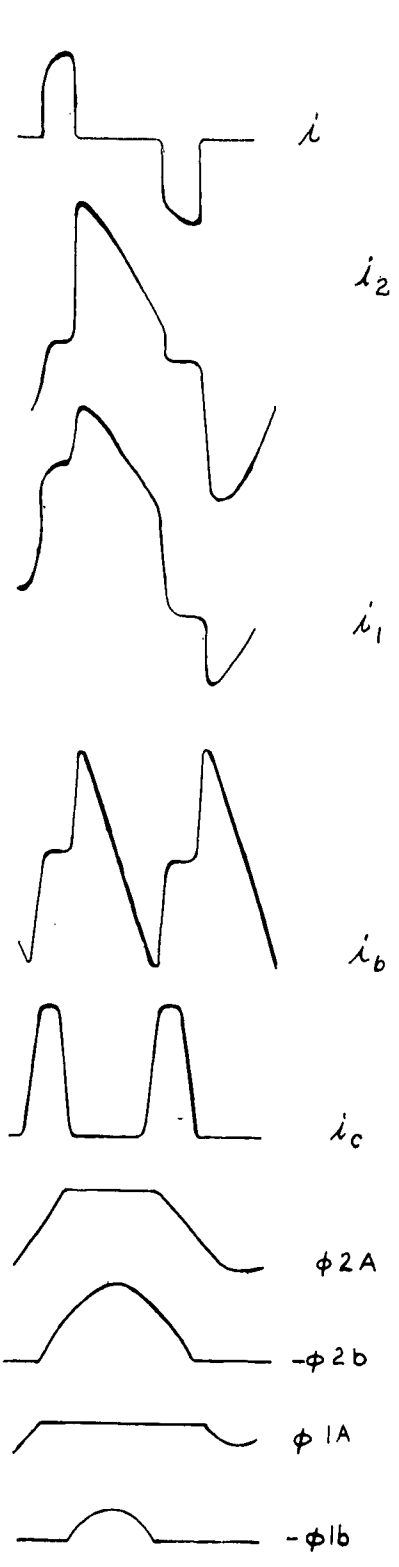

A.

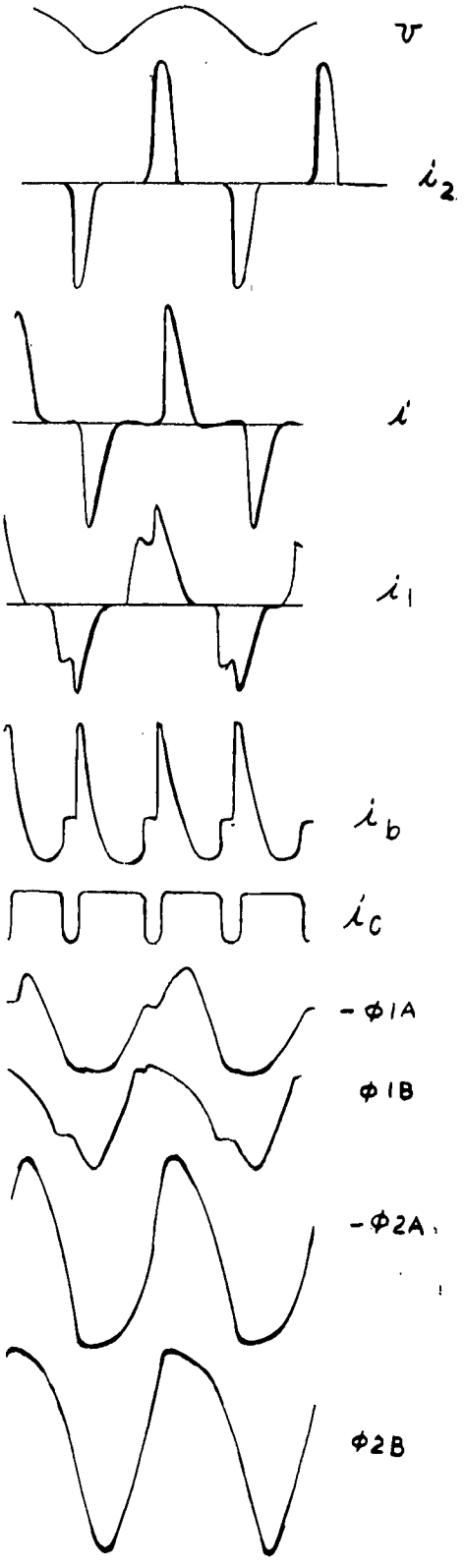

B.

MRI-13396

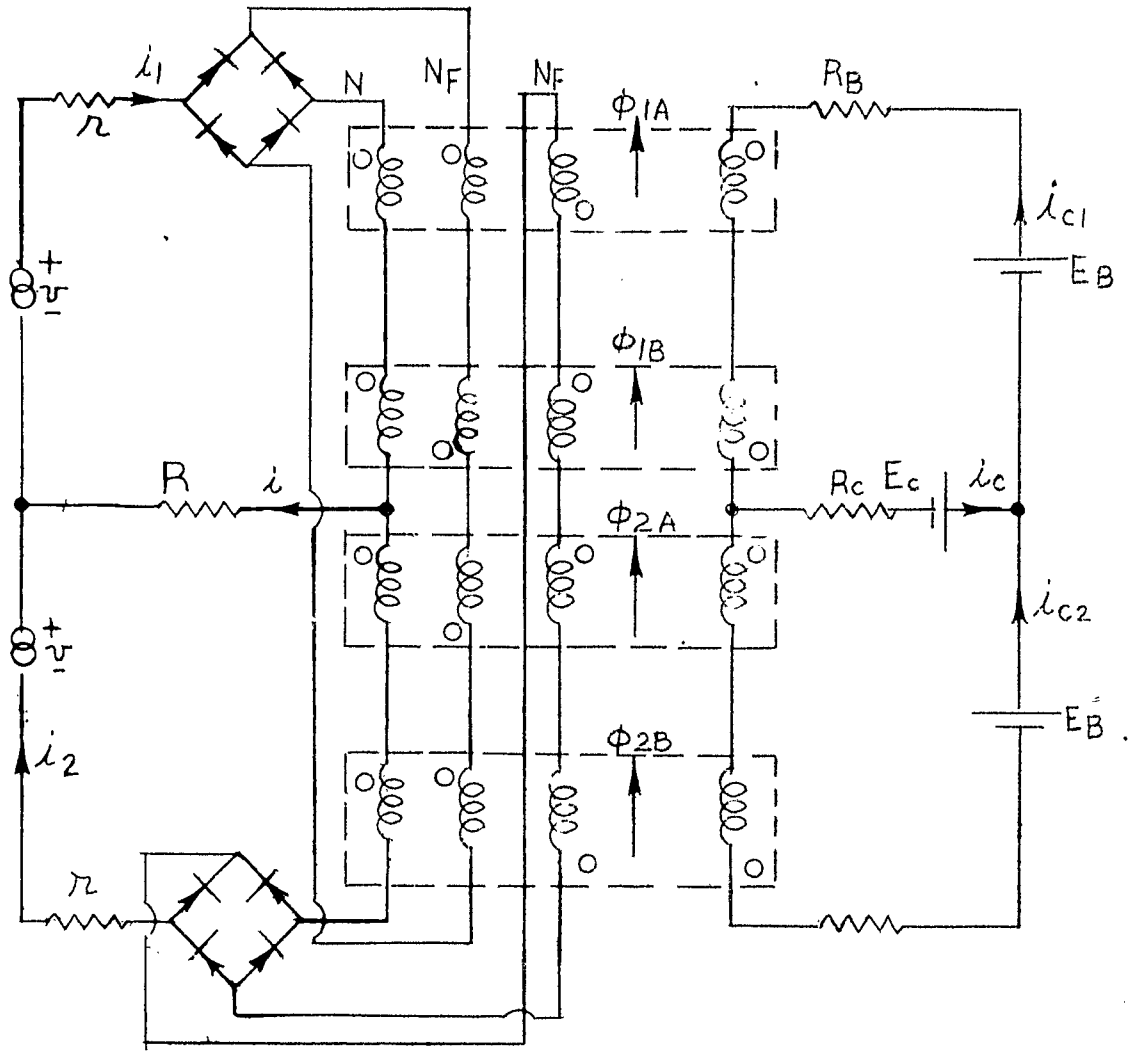

THE SPLIT-FEEDBACK PUSH-PULL AMPLIFIER

A.

MRI - 13397

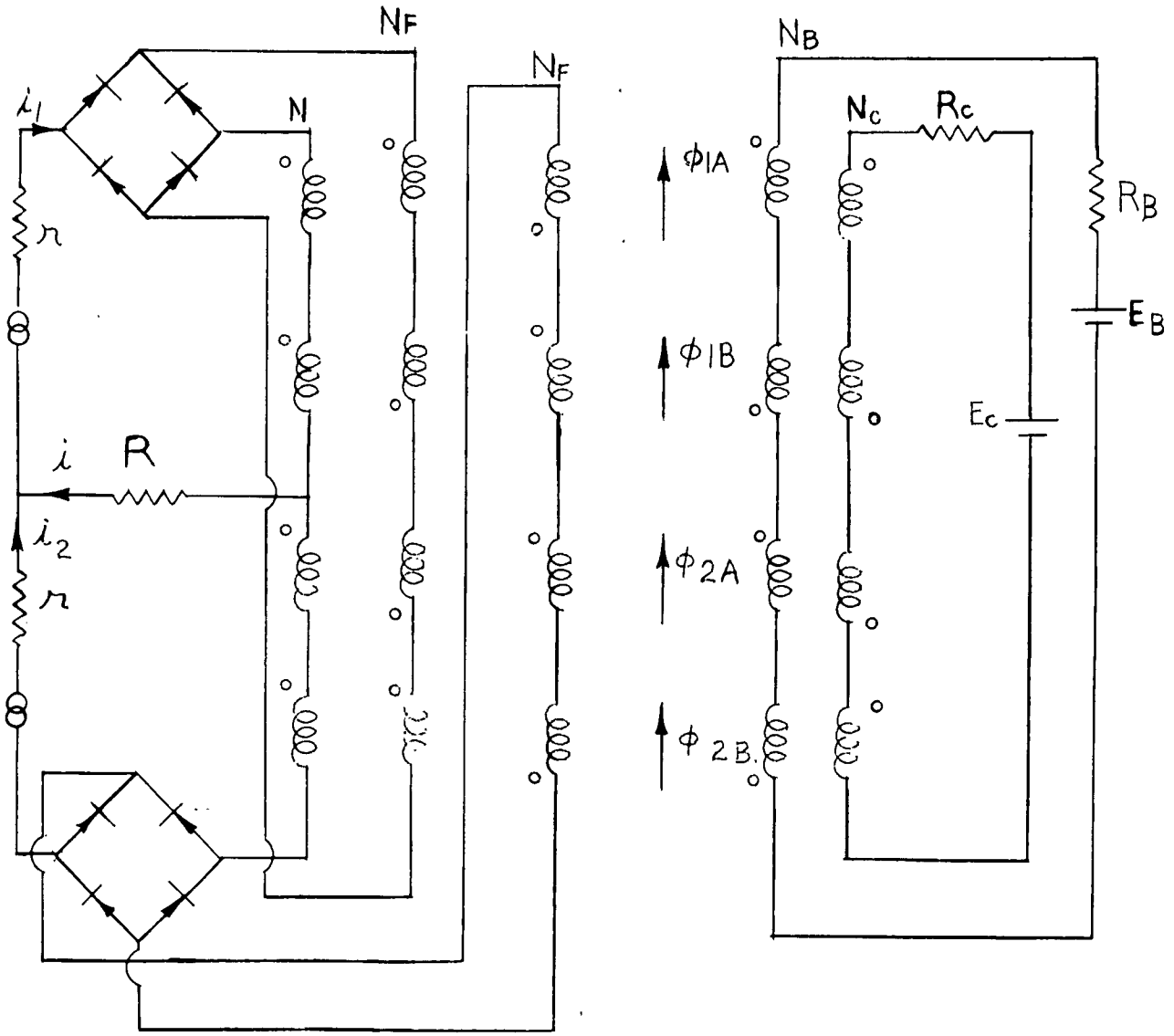

B.

THE SPLIT-FEEDBACK PUSH-PULL AMPLIFIER
SEPARATE CONTROL AND BIAS WINDINGS.

MRI-13398

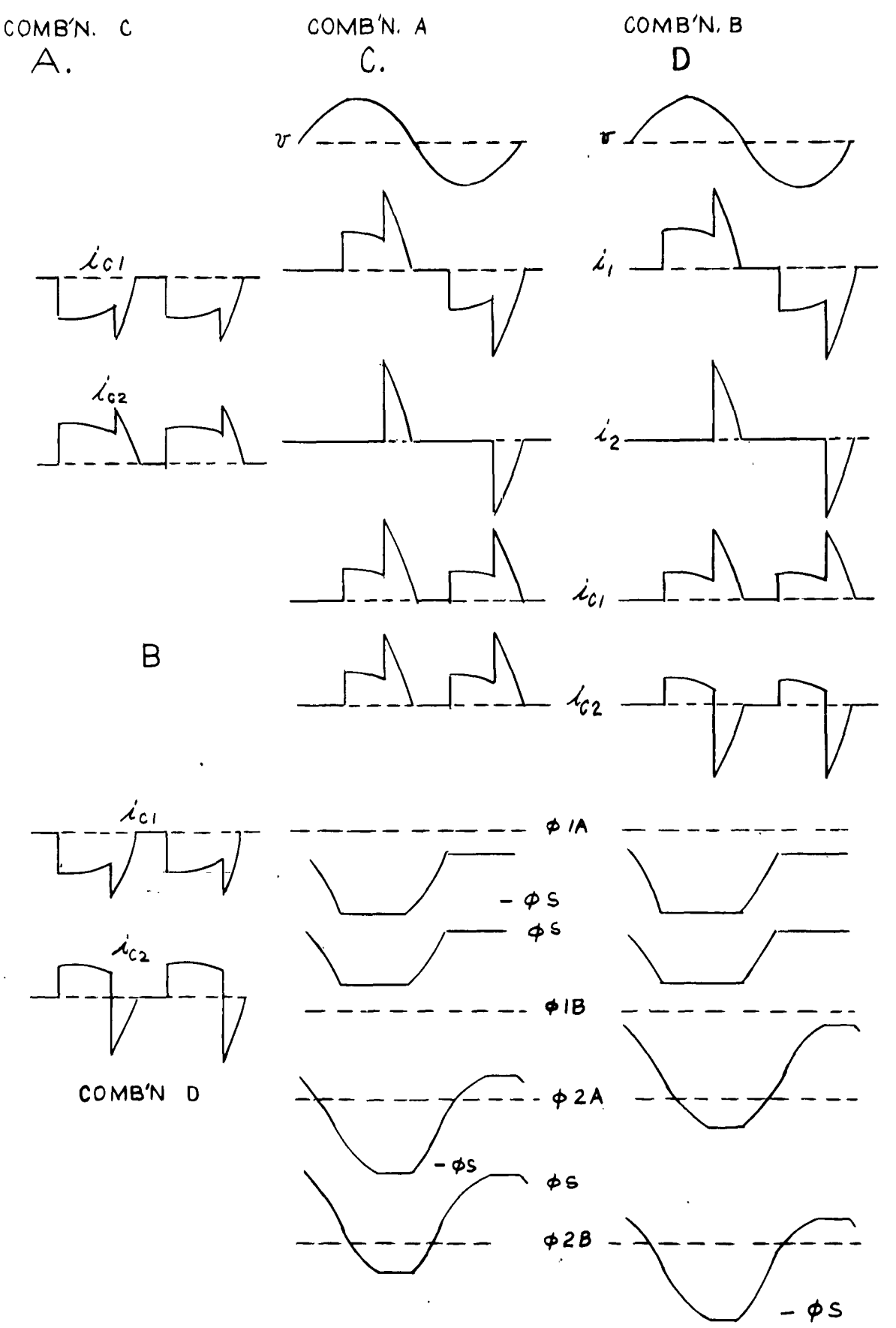
COMB'N. C
A.
COMB'N. A
C.
COMB'N. B
D
v
v
i_{C1}
i_1
i_{C2}
i_2
i_{C1}
B
i_{C2}
i_{C1}
i_{C2}
COMB'N D
ϕ 1A
$-\phi S$
ϕS
ϕ 1B
ϕ 2A
$-\phi S$
ϕS
ϕ 2B
$-\phi S$

MR1-13399

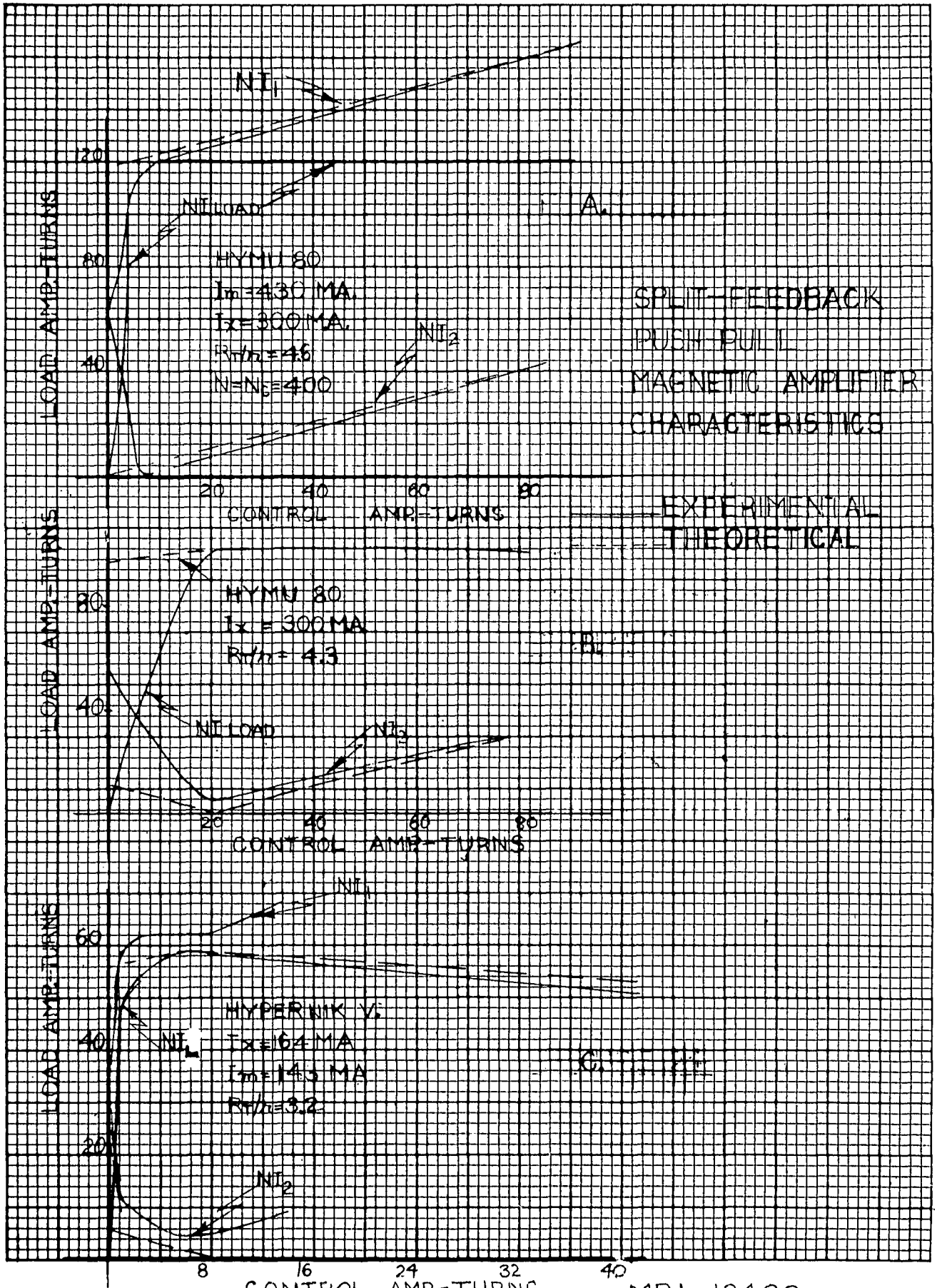
SPLIT-FEEDBACK
PUSH-PULL
MAGNETIC AMPLIFIER
CHARACTERISTICS
EXPERIMENTAL
THEORETICAL
A.
B.
C.
NI1
NIL LOAD
NI2
HYMU 80
Im = 430 MA.
Ix = 300 MA.
Rf/h = 4.6
N = N2 = 400
HYMU 80
Ix = 300 MA.
Rf/h = 4.3
NIL LOAD
HYPERNIK V.
Ix = 164 MA.
Im = 14.3 MA.
Rf/h = 3.2
LOAD AMP.-TURNS
CONTROL AMP.-TURNS
20
40
60
80
120
8
16
24
32
40

MRI-13400

SPLIT-FEEDBACK AMPLIFIER WAVEFORMS

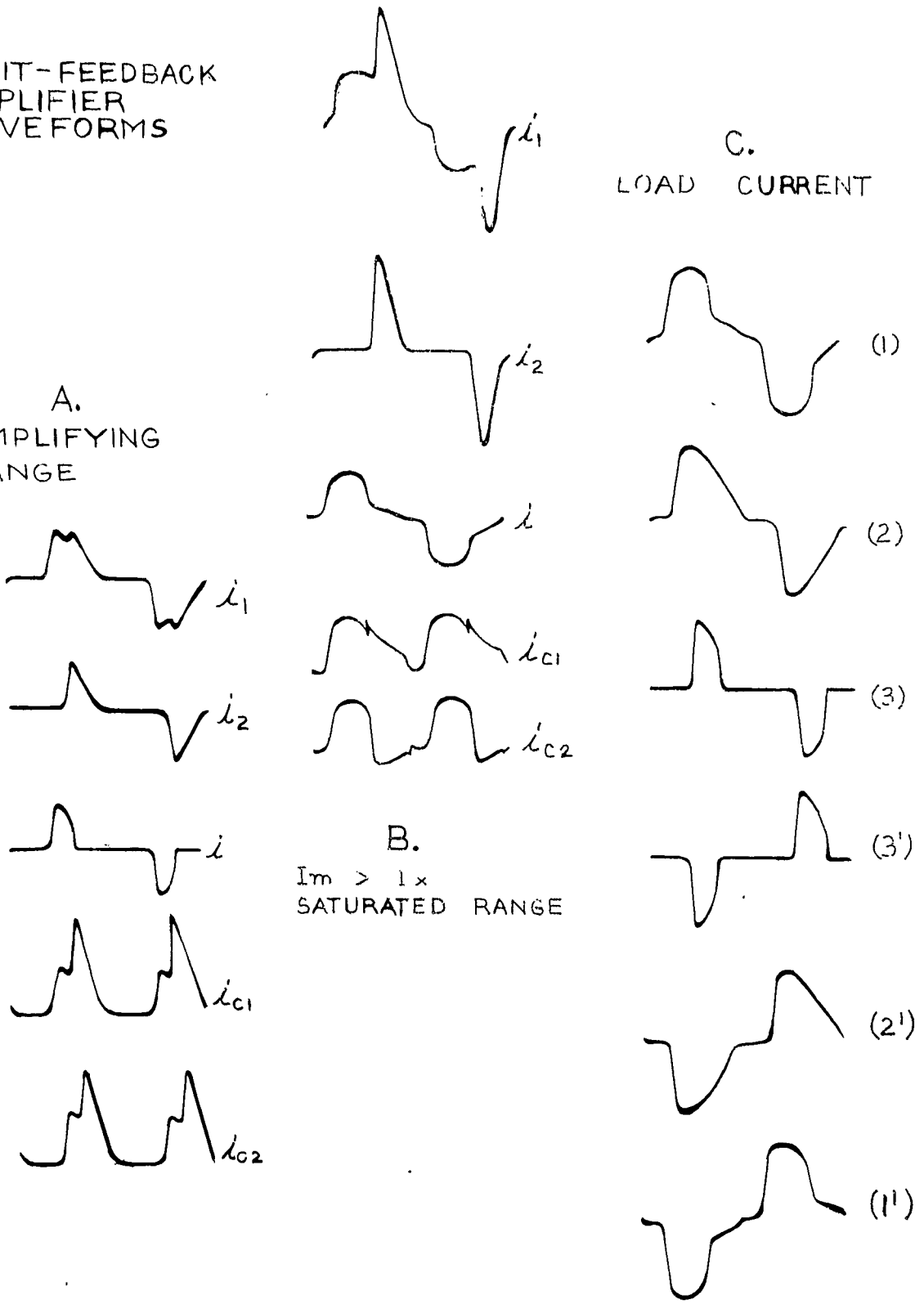

MRI-13401

Im < I_x - END OF AMPLIFYING RANGE

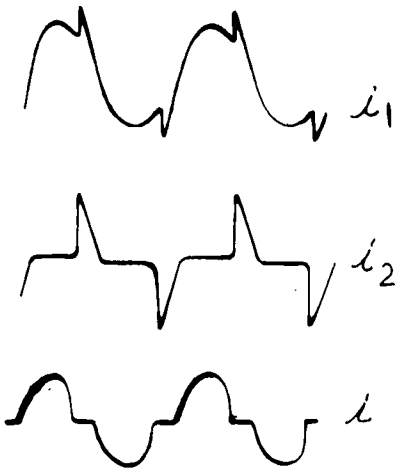

A.

Im < I_x - SAT. REGION

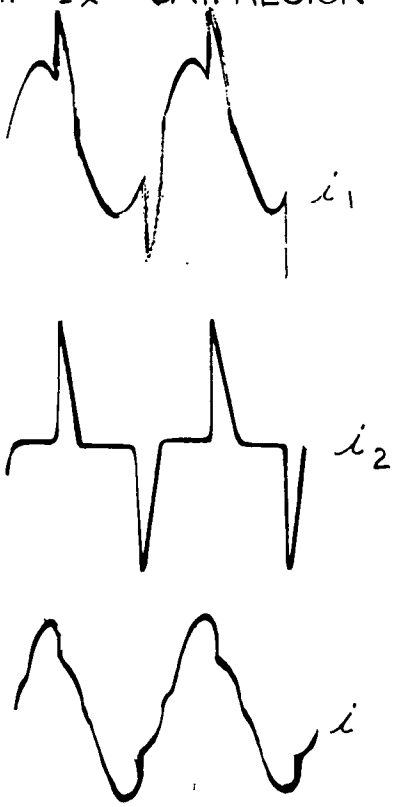

B.

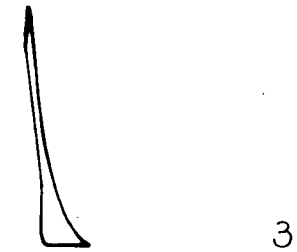

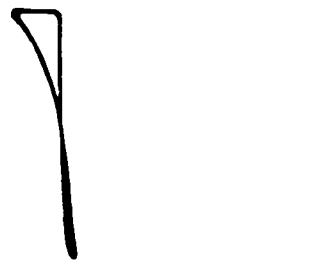

C.
B-H LOOPS

MRI - 13402

A. SERIES FEEDBACK AMPLIFIER

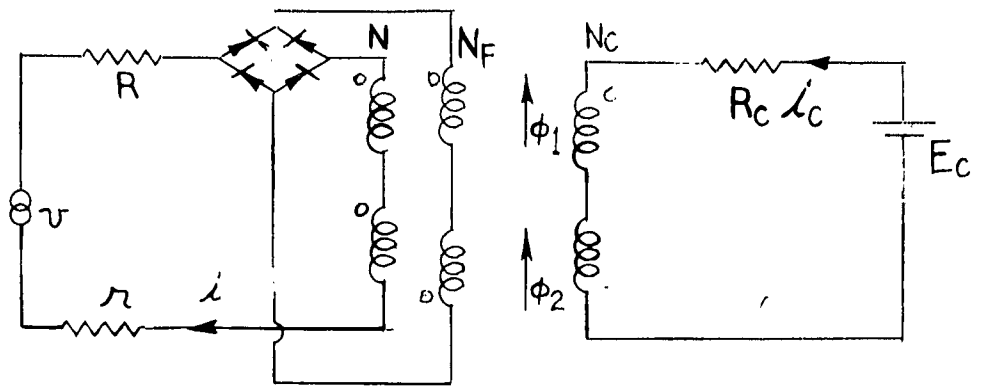

B.

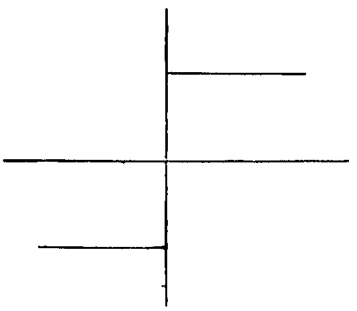

IDEAL B-H CHARACTERISTIC

C.

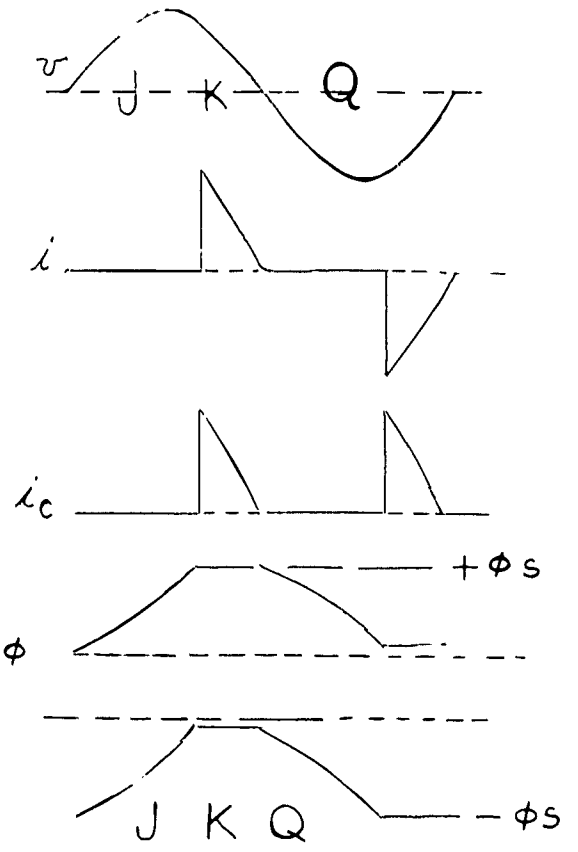

THEORETICAL WAVEFORMS

MRI - 13403

a

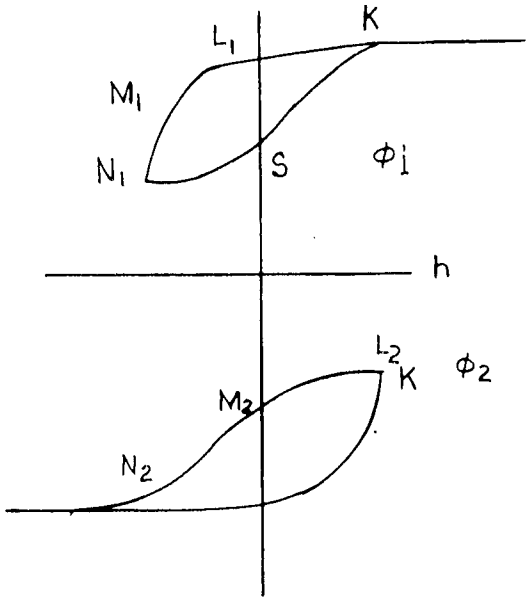

'ACTUAL'

b

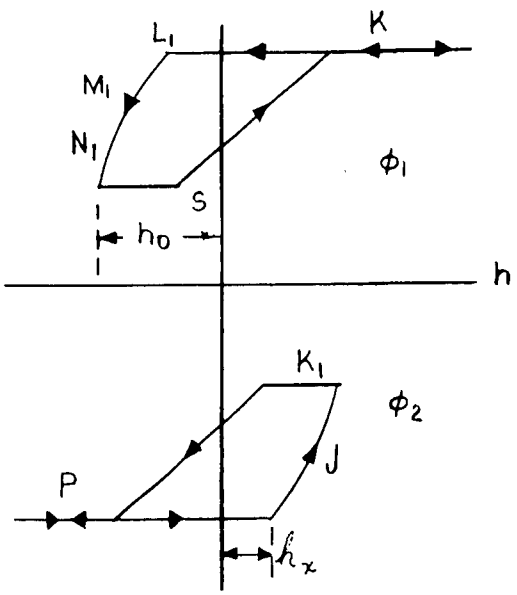

SIMPLIFIED

c

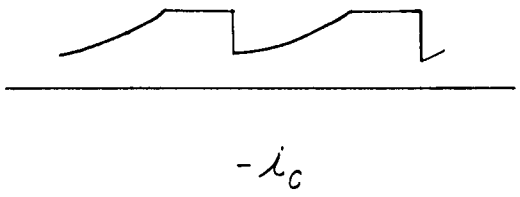

$-i_c$

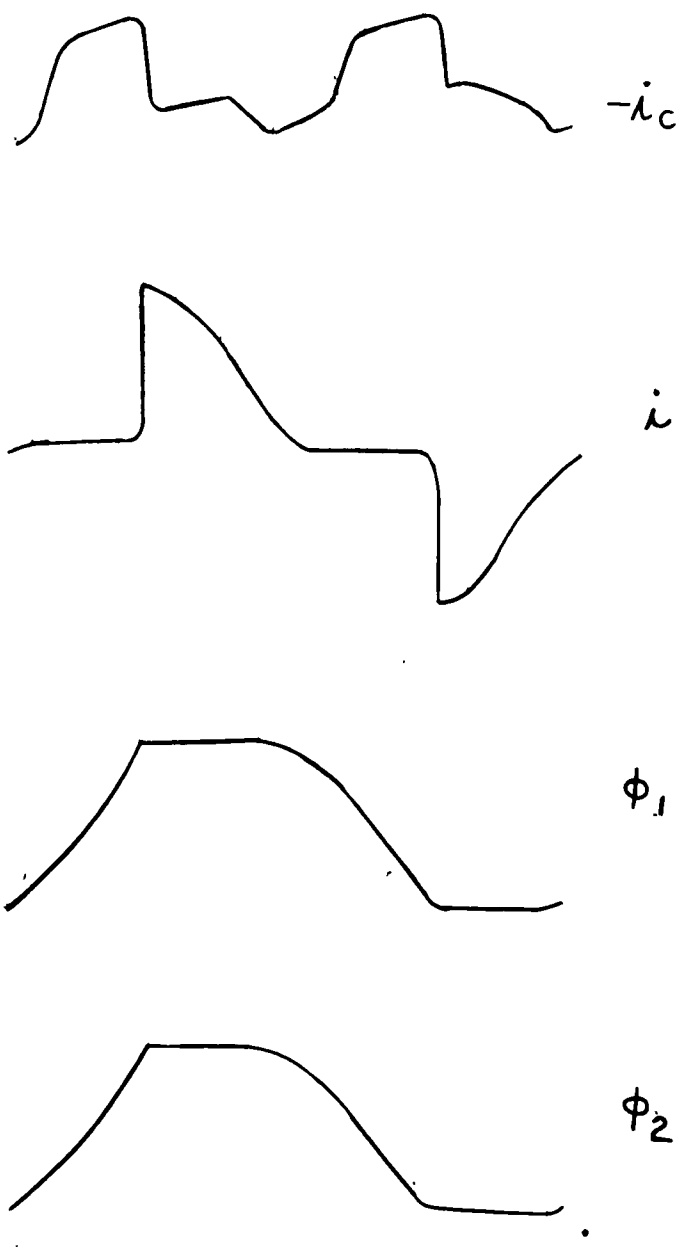

EXPERIMENTAL S.F. WAVEFORMS

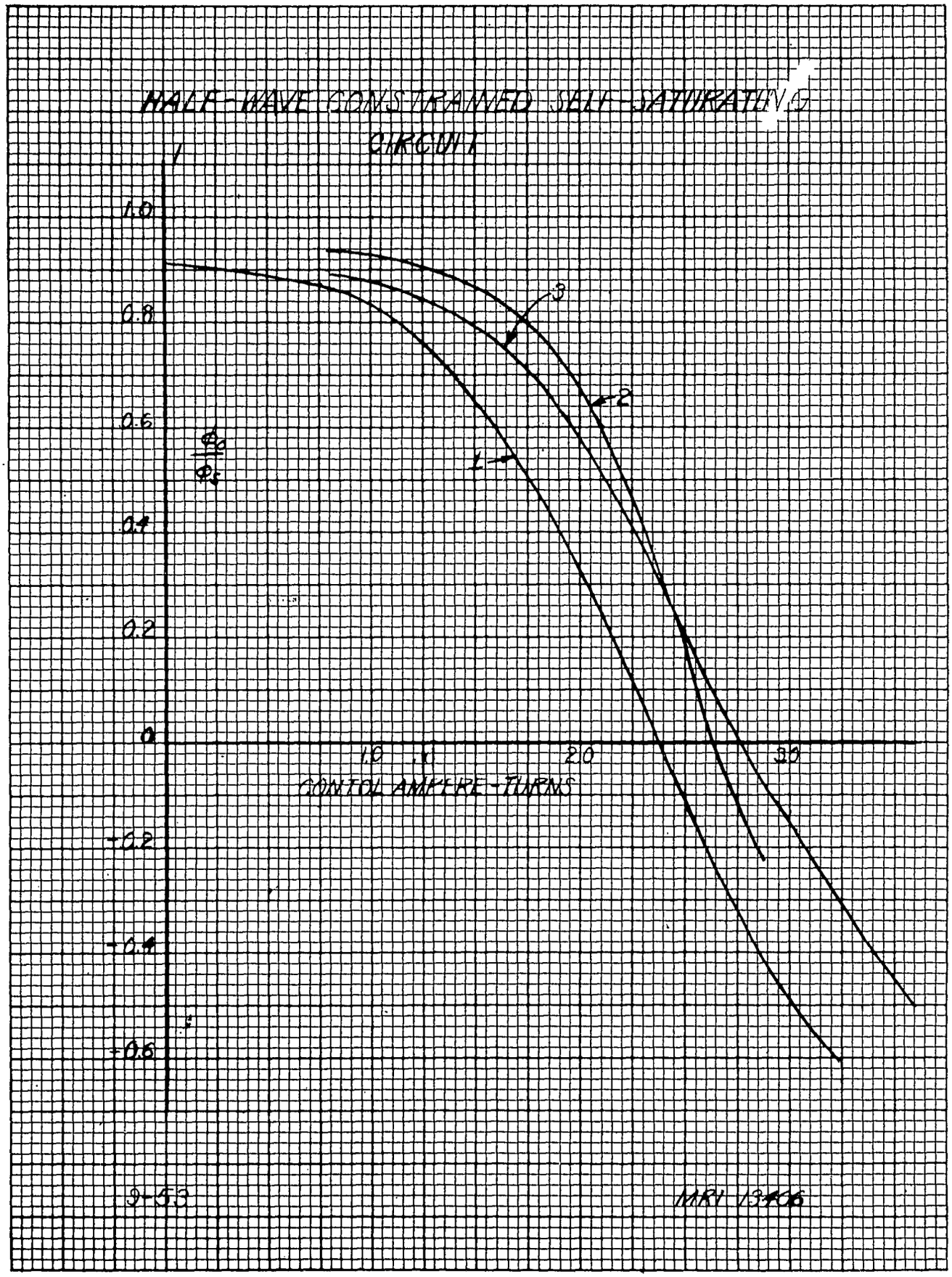
HALF-WAVE CONSTRAINED SELF-SATURATING CIRCUIT
1.0
0.8
0.6
0.4
0.2
0
-0.2
-0.4
-0.6
$\frac{\phi_0}{\phi_s}$
1
2
3
10
20
30
CONTOL AMPERE-TURNS
9-53
MRV 13466

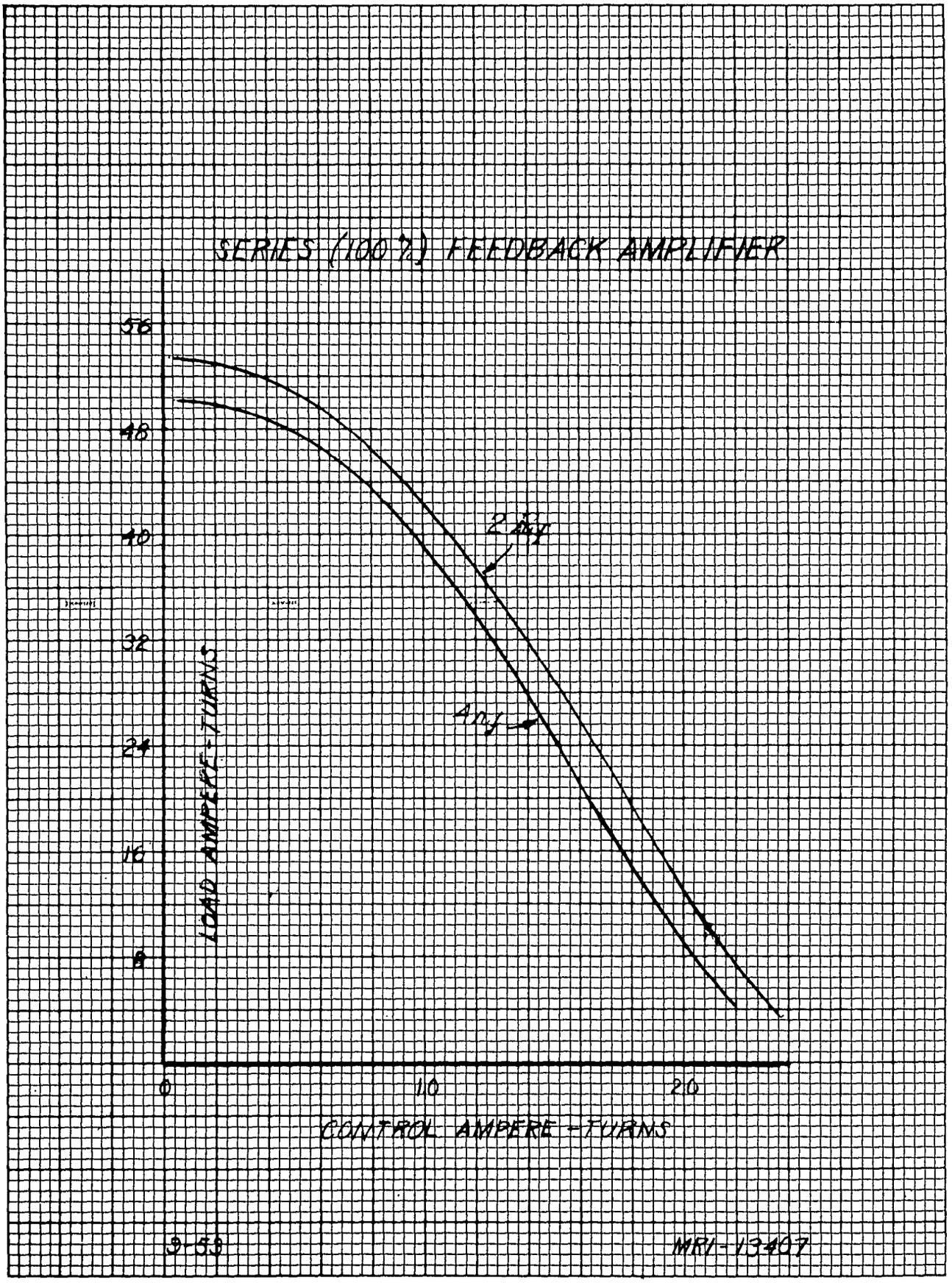
SERIES (100%) FEEDBACK AMPLIFIER
56
48
40
32
24
16
8
0
10
20
LOAD AMPERE-TURNS
CONTROL AMPERE-TURNS
2 ohms
4 ohms
3-53
MRI-13407

a

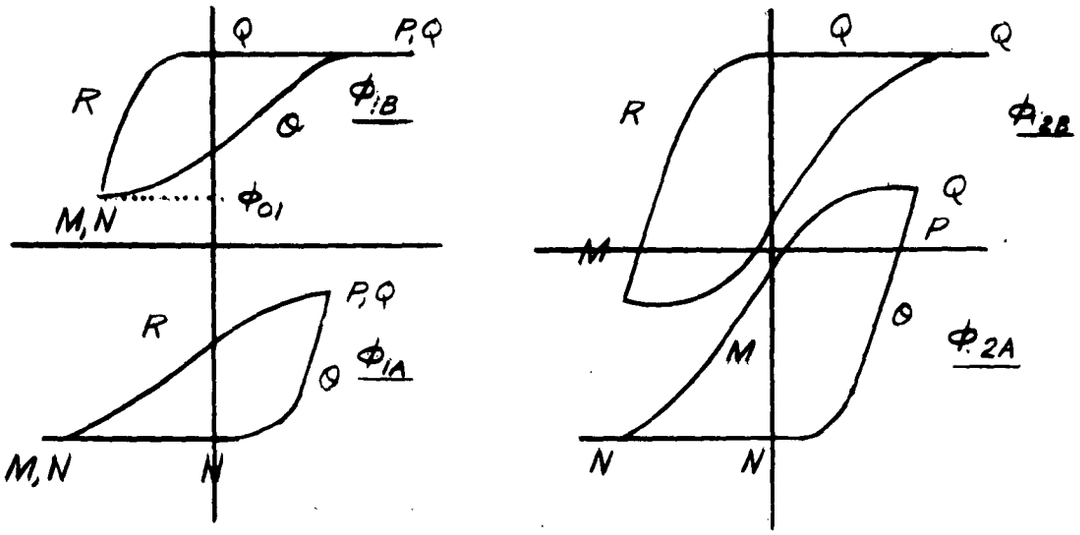

MINOR LOOPS - 'ACTUAL'

b

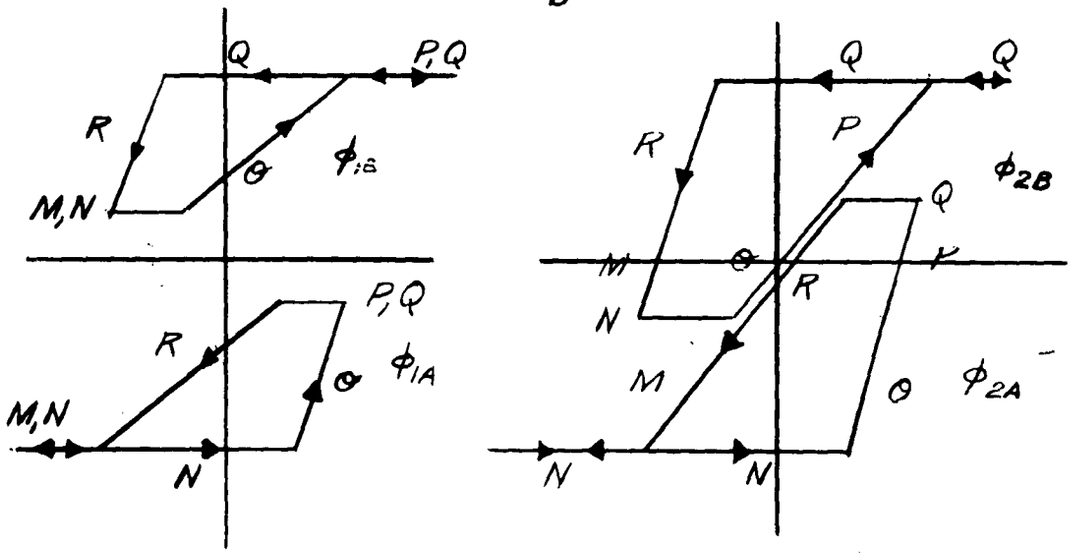

MINOR LOOPS - SIMPLIFIED

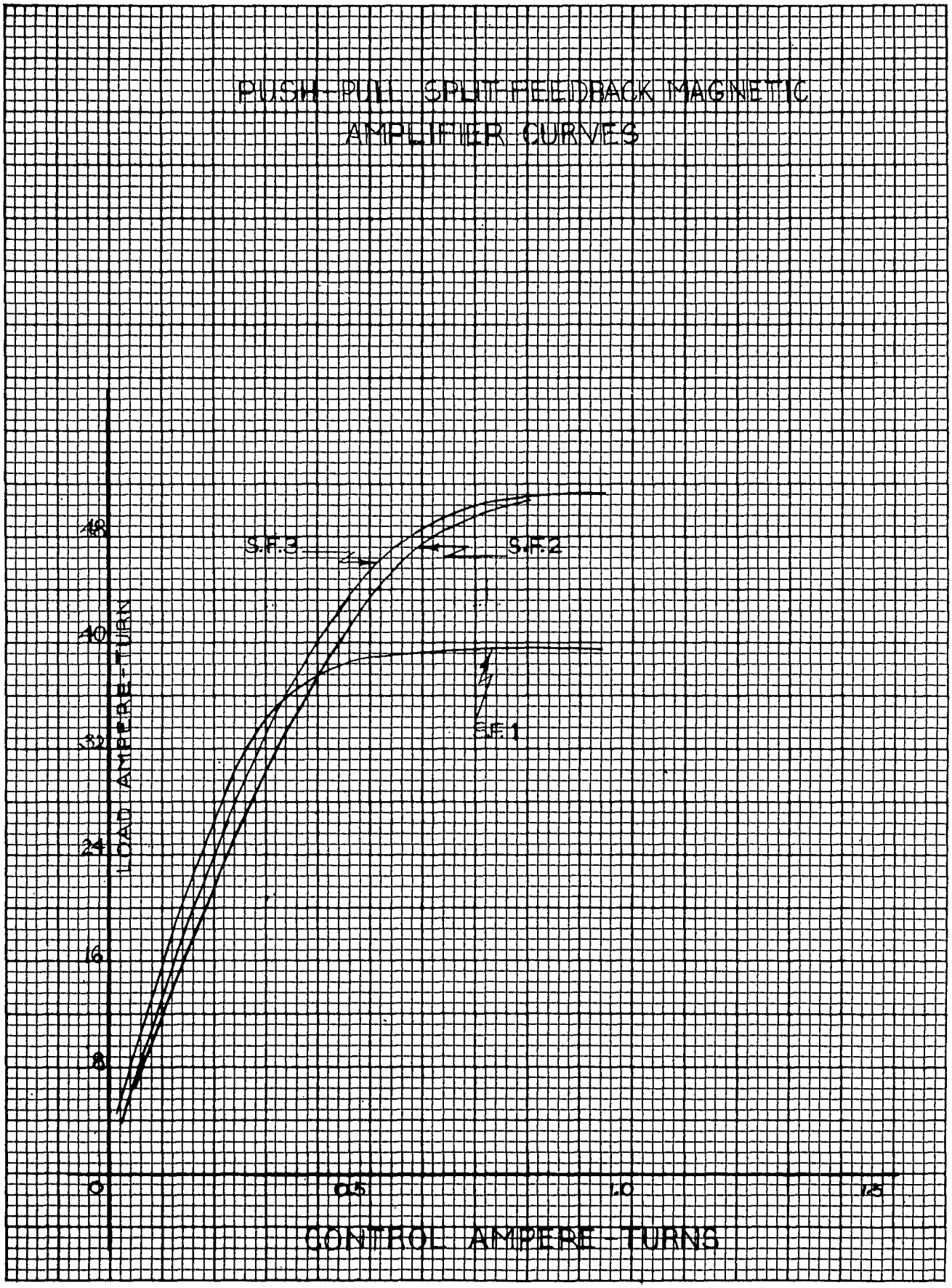
PUSH-PULL SPLIT-FEEDBACK MAGNETIC AMPLIFIER CURVES
48
40
32
24
16
8
0
LOAD CURRENT - MILLIAMPERES
S.F.3
S.F.2
S.F.1
0.5
1.0
1.5
CONTROL AMPERE-TURNS

MRI-13409

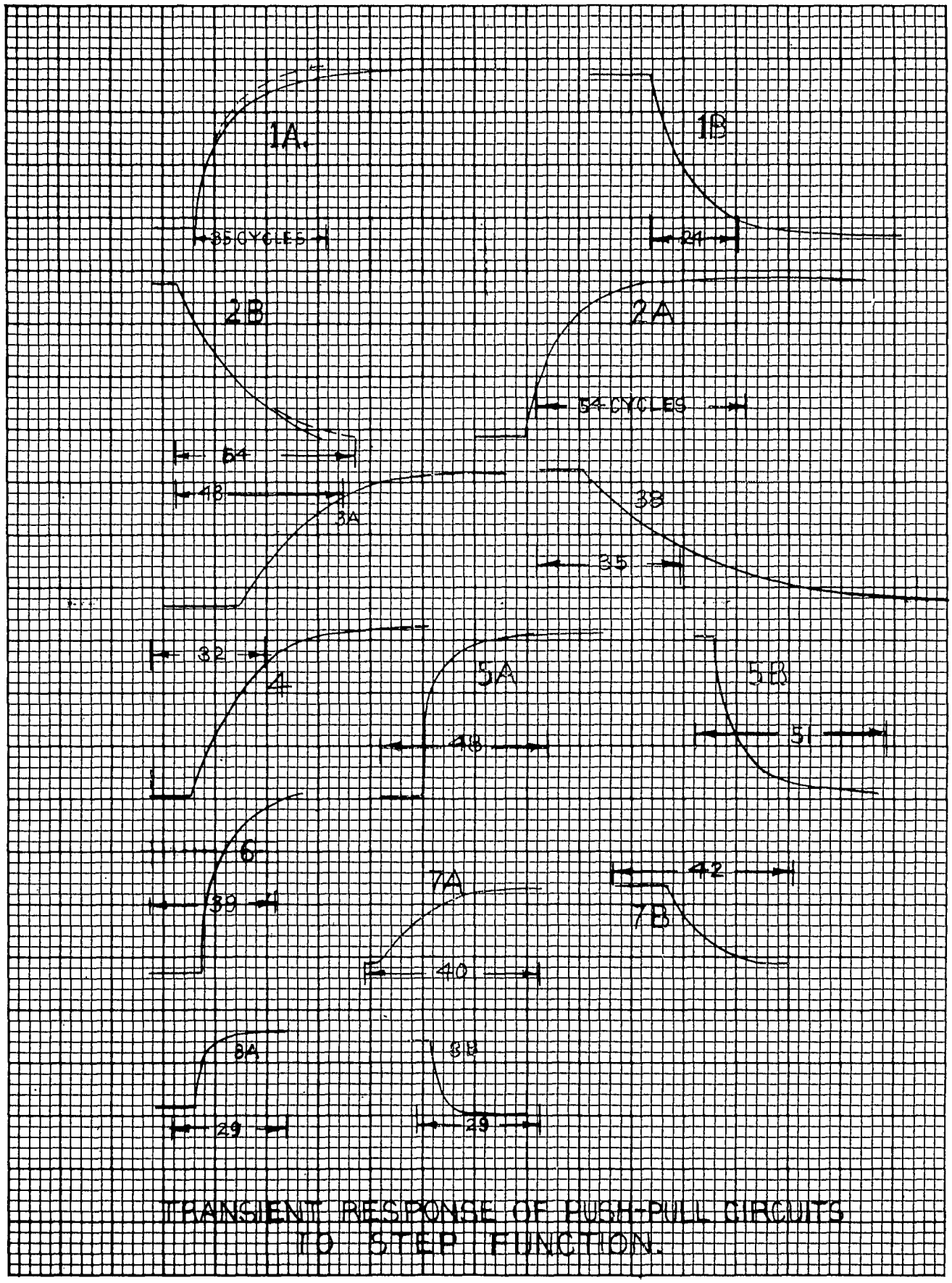

TRANSIENT RESPONSE OF PUSH-PULL CIRCUITS TO STEP FUNCTION.

MRI - 13410

A. PUSH-PULL VOLTAGE DOUBLER

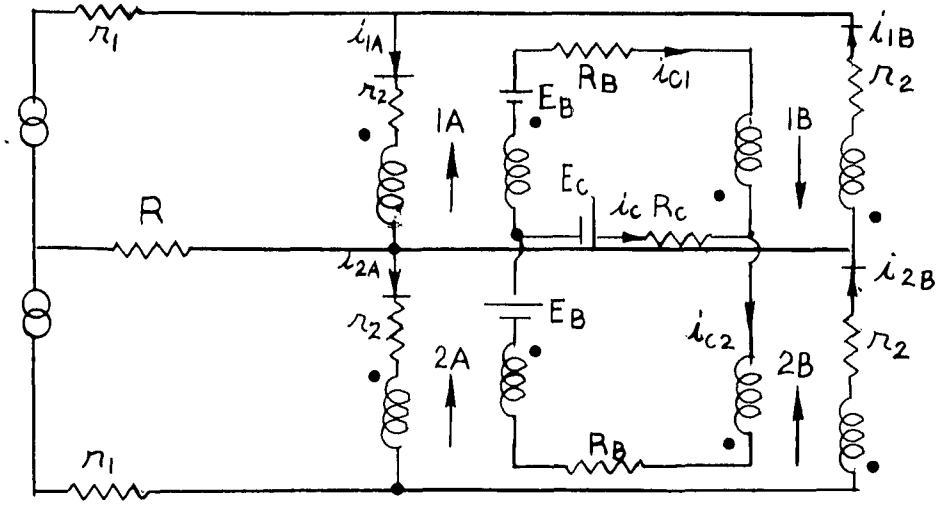

B. IDEALIZED MINOR B-H LOOPS

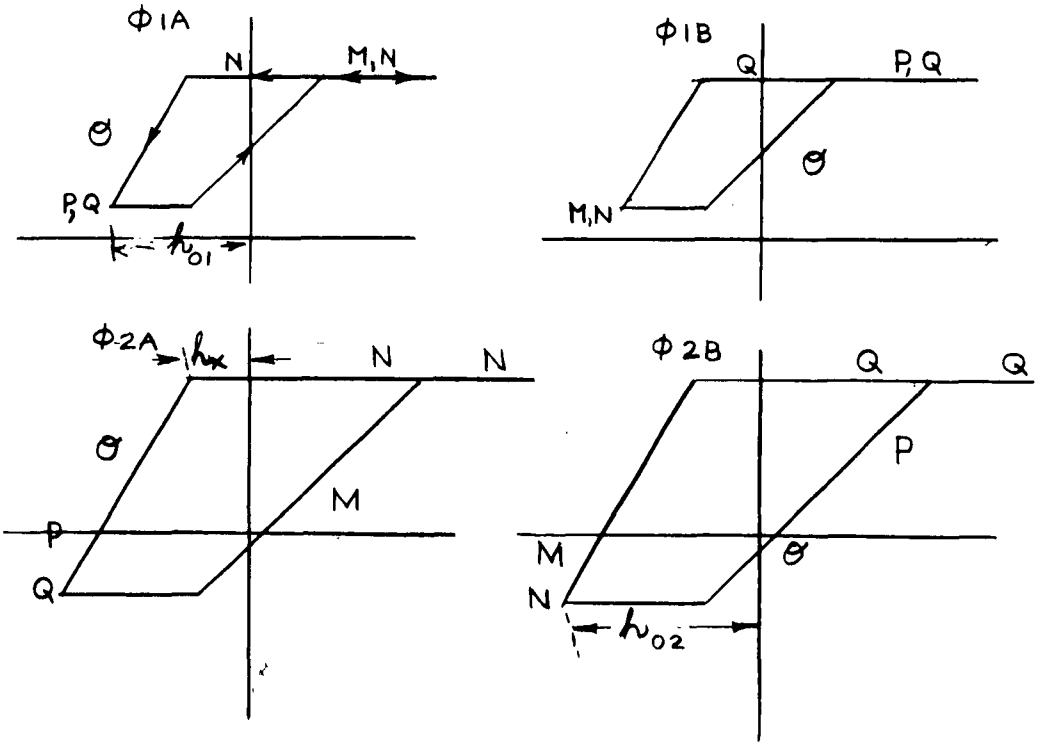

MRI-13411

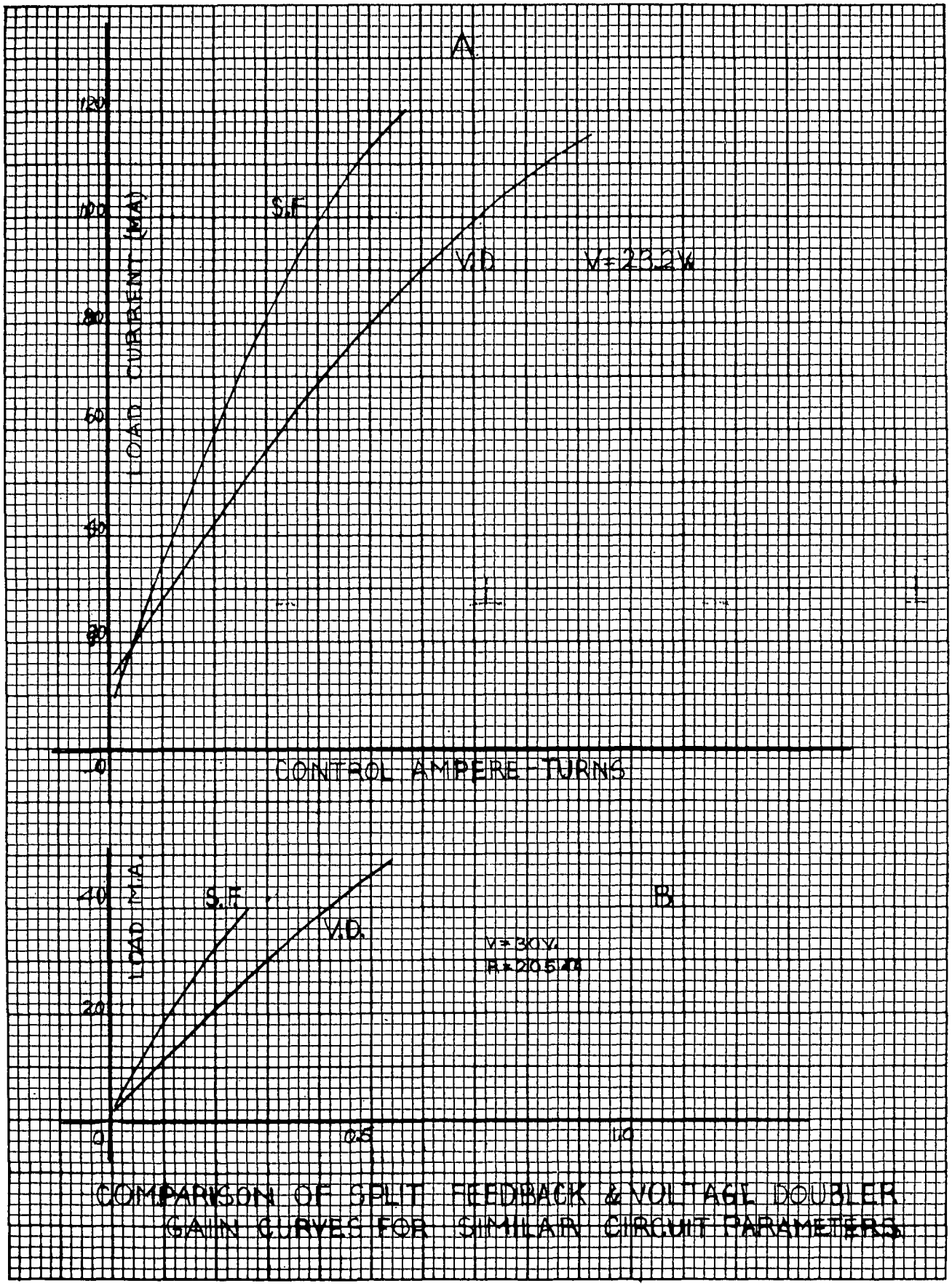

COMPARISON OF SPLIT FEEDBACK & VOLTAGE DOUBLER GAIN CURVES FOR SIMILAR CIRCUIT PARAMETERS.

MRI-13412

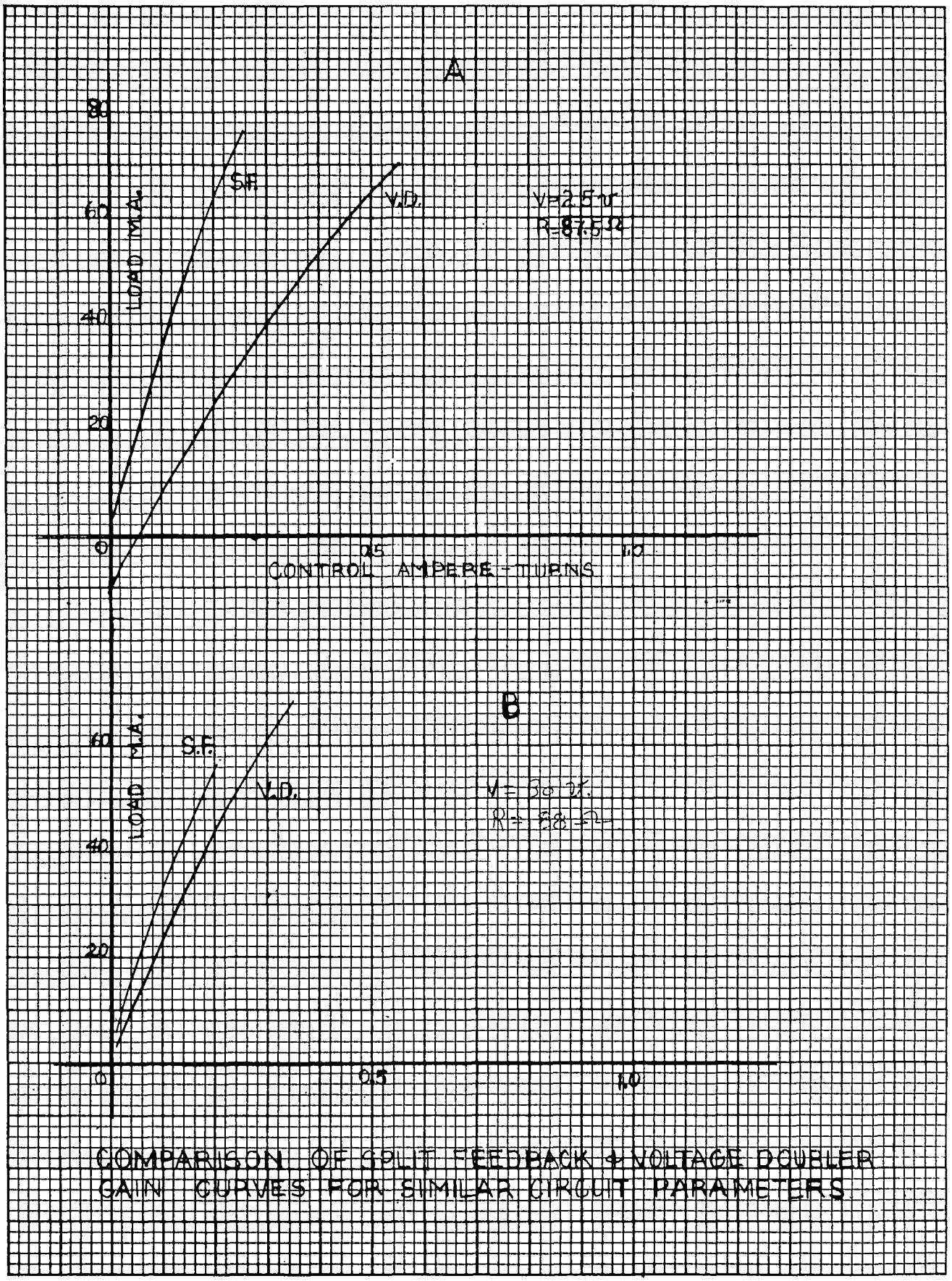

COMPARISON OF SPLIT FEEDBACK & VOLTAGE DOUBLER GAIN CURVES FOR SIMILAR CIRCUIT PARAMETERS

MRI-13413